UNIVERSITY OF CALIFORNIA,
IRVINE

Investigation of Cell-Cell Interactions in Development and Cancer Using a Microfabricated Co-culture Platform

DISSERTATION

Submitted in partial satisfaction of the requirements
for the degree of

DOCTOR OF PHILOSOPHY

In Biomedical Engineering

By

Katrina Marie Spencer

Dissertation Committee:
Assistant Professor Elliot Hui, Chair
Professor Christopher Hughes
Assistant Professor Wendy Liu
Professor Marian Waterman

2014

DEDICATION

to all of the wonderful people in my life, my family and friends.

TABLE OF CONTENTS

LIST OF FIGURES

LIST OF TABLES

ACKNOWLEDGEMENTS

I would like to thank all of those who have helped me in this endeavor:

To my advisor, Dr. Elliot Hui, for giving me this opportunity and for being such a dedicated mentor throughout this process.

To Drs. Chris Hughes, Wendy Liu, and Marian Waterman, for their valuable guidance and encouragement.

To my friends and family, for their continued support and for making this such a wonderful experience.

To Brian and Silas, for being my inspiration.

CURRICULUM VITAE

Katrina Marie Spencer

EDUCATION

2014	Ph.D. in Biomedical Engineering, University of California, Irvine
2013	M.S. in Biomedical Engineering, University of California, Irvine
2009	B.S. in Biology/Biotechnology, Cabrini College B.S. in Mathematics, Cabrini College
2008	Study Abroad, Stevenson College of Edinburgh, Scotland

RESEARCH EXPERIENCE

2010-2014	Graduate Student Researcher UC Irvine, Advisor: Dr. Elliot Hui
2008	Research Fellow U.S. Department of Energy, Advisor: Dr. Jessica Hellman
2007-2009	Undergraduate Researcher Cabrini College, Advisor: Dr. Sheryl Fuller-Espie
2007-2009	Undergraduate Researcher Cabrini College, Advisor: Dr. John Brown
2007	Research Intern Merck Animal Health-Research & Development Bateriology Lab

PUBLICATIONS
[* Denotes equal contribution to work]

Spencer, K. H., Kim, M. Y., Hughes, C. C. W., Hui, E. E. (2014). A Screen for Short-Range Paracrine Interactions. *Integrative Biology 6* (4), 382-287. **[Cover Article]**

*Thompson, N. G., ***Spencer, K. H.**, Hui, E. E., & Lock, L. (Under Review). Microfabricated substrate supports mouse embryonic stem cell growth and yields highly pure stem cell populations.

Rao, N., Grover, G. N., Vincent, L. G., Evans, S. C., Choi, Y. S., **Spencer, K. H.**, Hui, E. E., Engler, A. J., Christman, K. L. (2013). A co-culture device with a tunable stiffness to understand combinatorial cell-cell and cell-matrix interactions. *Integrative Biology 5* (11), 1344-1354. **[Cover Article]**

Rao, N., Evans, S., Stewart, D., **Spencer, K. H.**, Sheikh, F., Hui, E. E., and Christman, K. L. (2013). Fibroblasts influence muscle progenitor differentiation and alignment in contact independent and dependent manners in organized co-culture devices. *Biomedical Microdevices 15* (1), 161-169.

Fuller-Espie, S. L., *Goodfield, L., ***Hill, K.**, Grant, K., and DeRogatis, N. (2008). Conservation of cytokine-mediated responses in innate immunity: a flow cytometric study investigating the effects of human proinflammatory cytokines on phagocytosis in the earthworm *Eisenia hortensis*. *Invertebrate Survival Journal*, *5*, 124-134.

AWARDS AND HONORS

2014	Toastmasters Distinguished Member Award
2014	UC Irvine Graduate Student Research and Travel Grant
2011	NSF Graduate Research Fellowship
2010	Center for Complex Biological Systems Opportunity Award Research Grant
2009	Howard Hughes Medical Institute Fellowship
2009	Biology Departmental Award
2009	Mathematics Departmental Award
2008	Pennsylvania Academy of Sciences Student Research Grant

ABSTRACT OF THE DISSERTATION

Investigation of Cell-Cell Interactions in Development and Cancer Using a Microfabricated Co-culture Platform

By

Katrina Marie Spencer

Doctor of Philosophy in Biomedical Engineering

University of California, Irvine, 2014

Professor Elliot E. Hui, Chair

Communication between heterogeneous populations of cells within a tissue dictate the overall function of the tissue and is often disregulated in disease states. This crosstalk can be quite complex and difficult to study. We investigate heterotypic cell-cell signaling using a microfabricated co-culture system that allows us to easily purify each population following co-culture for independent analysis and to rapidly manipulate the populations so that even very brief co-cultures can be precisely achieved. The devices are also designed so that the populations can be co-cultured in close proximity for maximum exchange to occur. We have previously used this platform to study the maintenance or differentiation of various types of stem and progenitor cells. In this current work we use the co-culture system to develop a high-throughput screening technique for short-range paracrine interactions. The platform was also utilized in conjunction with conventional tools to study the effects of tumor-stromal interactions on fibroblast migration. We found that colon cancer cells induce colon fibroblast migration through a mechanism involving canonical WNT signaling and urokinase-type plasminogen activator (uPA) induction. These findings

are crucial to understanding how tumor cells recruit stromal cells into the tumor microenvironment to promote cancer progression. In addition to making the short-range screening platform, we also created an experimental model for morphogen-dependent border formation in the developing telencephalon using the comb system and began to study the effects of BMP and FGF signaling interactions on dissociated cortical precursor cells (dCPC). Finally, we developed a method of maintaining mouse embryonic stem cells (mESC) that facilates easy extration of pure mESCs populations from culture with feeder cells. In doing so, we showed that maintenance of stem cell markers in feeder-dependent mESCs may not require direct contact with feeders, as was previously thought, but rather only appears to require close-proximity paracrine communicaiton with feeders.

Introduction

Cellular interactions

Organ and tissue function is dependent on the complex arrangement of cells within them and the coordinated cellular behavior that this organization causes. The cellular organization determines how the individual cells will communicate with their environment and with each other and, upon interpretation of these external signals, the cells respond with behavior changes involving altered protein expression and activity. Cells use communication including juxtacrine, paracrine, and autocrine signaling to sense the state of their environment and this triggers downstream intercellular signaling pathway activation to determine the appropriate cellular response.

Juxtacrine Signaling

Juxtacrine signaling involves the physical contact between a cell and its neighbor or between a cell and the extracellular matrix (ECM) in its environment. The first type of cell-cell juxtacrine signaling requires the binding of a membrane-bound protein receptor to a membrane-bound protein ligand on an adjacent cell. The conformational change in the receptor induced by the binding event initiates a cascade of intercellular protein interactions. Canonical Notch signaling is one example of this form of juxtacrine communication. Delta, Jagged, or Serrate proteins displayed by one cell bind to the extracellular portion of one of four Notch receptors on a neighboring cell, which results in cleavage of the receptor to release the Notch intracellular domain (NCID) and allow for its nuclear translocation and induction of target gene expression.[1] Notch signaling is know for its role in driving binary cell fate decisions among cells with similar fate potentials and for

generating complex patterns in tissues with diverse cell types.[1] Cadhereins are transmembrane proteins that also mediate cell-cell interactions. The binding of cadherins on adjacent cells regulates cell-cell adhesion and migration by affecting cytoskeleton dynamics, and causes cell sorting in development.[2] Neural cadherin (N-Cad) has even been shown to activate fibroblast growth factor receptor (FGFR) in the absence of its conventional ligand FGF to induce mitogen-activated protein kinase-extracellular signal-related kinase (MAPK-ERK) signaling.[3]

A second type of cell-cell juxtacrine communication can occur through gap junctions. Gap junctions are channels formed from connexin proteins that couple the cytoplasms of two neighboring cells and allow for the free exchange of small molecules or ions.[4] Gap junctions help to coordinate collections of cells and their importance has been demonstrated in normal tissue function, development, and cancer.[4-6] In smooth muscle, myocardium, and nerve tissue, electrical signals are transmitted throughout groups of cells, to synchronize electrical and mechanical output.[4]

In addition to that which occurs between adjacent cells, juxtacrine interactions can also occur between membrane-bound protein receptors, called integrins, on a cell and ECM components in its environment. Integrins, like cadherins, are linkers that connect the cytoskeleton to the ECM and transmit force across the plasma membrane to aid in migration and adhesion. The binding of integrins to macromolecules such as fibronectin, laminin, or collagen also actives various signaling pathways to effect proliferation and growth factor signaling, and to further modulate migration and adhesion.[7]

Soluble Factor Signaling

Aside from communication through physical contact with other cells or ECM, cells can also receive soluble signals from their environment. Cells can interact over long distances, through endocrine signaling, by secreting hormones into the blood. In contrast, paracrine communication involves small molecule or protein factors that are only effective over shorter distances. Upon secretion by effector cells, they affect target cells within the immediate vicinity by diffusing through their plasma membrane or binding to surface receptors. In contrast, autocrine signals are secreted and detected by the same cell. Some factors only act over very short distances because they are highly labile (e.g. reactive oxygen species, ROS),[8] are only effective at high concentrations (e.g. Nodal),[9] are easily trapped in ECM (e.g. fibroblast growth factor, FGF),[10] or may be anchored to the membrane through lipid modifications (e.g. WNTs).[11]

Many of the proteins that are soluble factors belong to the fibroblast growth factor (FGF) family, tumor growth factor beta (TGFβ) family, Hedgehog (HH) family, or Wingless (WNT) family. FGFs regulate processes including migration, proliferation, differentiation, and survival in development, tissue homeostasis, or disease by binding to FGF receptors (FGFR) to activate pathways involving Jun N-terminal kinase (JNK), Ras, mitogen-activated protein kinases (MAPKs), and extracellular signal-regulated kinases (ERKs). They have high affinity for components of the ECM and thus can also be released upon degradation of the matrix. Like FGF, TGFβ and bone morphogenic proteins (BMP) mediate differentiation, proliferation, and survival, as well as ECM remodeling, in a number of different cell types through (Smad) and MAPK signaling. Hedgehog proteins regulate proliferation, cancer progression, and tissue patterning during development by binding to their receptor

Patched to activate target gene expression through Gli transcriptional activators. WNTs regulate migration, proliferation, differentiation, survival, and cancer progression, as well, and act by binding to frizzled (FZD) receptors to induce beta catenin-mediated transcriptional activation. WNT and HH proteins possess hydrophobic modifications that restrict their range of diffusion. However, the hydrophobic portions can be shielded by lipid-binding proteins, by forming complexes of multiple WNT or HH proteins, or by traveling on exosomes[11] and this extends their signaling range.

Co-culture Methods

In order to better understand these cell-cell interactions to further our knowledge of tissue function and disease progression, it has been quite effective to study them in simpler and highly controlled settings *in vitro.*[12-16] The numerous culture methods differ in the number of cell populations they include, the spatial organization of the populations, and the amount and type of communication that populations are able to exchange.

Unpatterned Culture

The early culture studies investigated cell behavior in monoculture, in which a single population of cells was grown in a tissue culture dish. Because tissues are generally composed of multiple cell types that cooperate together to determine tissue function, this approach can provide some insight on the function of a cell type when it is alone, but cannot mimic the behavior of the cell type in the complex tissue. Thus other studies used mixed co-cultures, in which multiple cell populations were seeded into dishes and were allowed to participate in heterotypic interactions. However, seeding cells into a normal tissue culture dish results in the random placement of cells along the bottom of the dish

and makes it difficult to regulate the degree of juxtacrine (and paracrine) signaling that occurs among the cells.

Patterned Culture

To study cellular crosstalk in a much more controlled manner, methods of spatially patterning cells in precise geometries have been developed. Many of these approaches use microfabrication techniques. Bhatia et al. (1999) patterned co-cultures of hepatocytes and fibroblasts. Collagen was patterned onto a borosilicate wafer using photolithography and, due to their selective adhesion to the collagen and not to the unpatterned wafer surface, hepatocytes adhered in the same pattern. Subsequently, fibroblasts adhered to the unpatterned areas of the wafer by adding serum during seeding.

Soft lithography has also been used to create stamps, stencils, and microfluidic devices to pattern proteins and cells for co-culture studies. Stamps made of poly(dimethylsiloxane) (PDMS) and exhibiting patterns in relief can be inked with proteins and placed on a surface to transfer the proteins and determine the location of cell adhesion.[17] In addition, stamp features can be also used to block protein and cell adhesion on specific areas of a substrate.[18] In a similar manner, thin PDMS or parylene stencils containing microfabricated holes can be applied to a surface to prevent protein and cell adhesion except for in the regions of the holes.[19] It can then be removed to allow a second cell type to attach to the remaining space.[20-22] By seeding the second cell type on the surface of the stencil, removing it after a given length of time, and seeding a third cell type in its place, dynamic co-culture is achievable.[23] Microfluidics has enabled multiple cell populations to be precisely patterned in adjacent channels or compartments that are

connected in order to permit crosstalk[24,25] or to be organized in spheroids using hydrodynamic focusing.[26]

In addition to heterotypic spheroids generated either in dishes or by microfluidics, other three-dimensional co-cultures of patterned cells have been used to investigate cellular communication. These often employ soft lithography as well. Cells are embedded in a matrix, which is then molded to a particular shape and combined with other molded matrices containing other cell populations.[27] While soft lithography has been useful in creating 3D co-cultures, the addition of complementary DNA sequences to the surface of cells has enable the creation of complex self-assembling cell aggregates.[28]

Indirect co-culture

While these co-culture methods can provide valuable information with regard to how cell communicate and affect each other's behavior, in many cases it is difficult to distinguish the effects of contact-dependent interactions from the effects of paracrine interactions, since the cell populations participate in both types during the co-culture. Methods exist that can be used for both contact co-culture and indirect co-culture, where the cell populations do not touch, so that the affects of the two types of communication can be distinguished. These are generally made using microfabrication, which may not be easily performed by some labs lacking the necessary expertise and clean room facilities. As a result, many investigations of paracrine communication are performed using simple techniques that only require commercially available materials. One of the most commonly used methods is conditioned media transfer. In this technique, one population of cells is cultured in a dish, and after a given length of time, the culture media, which is now conditioned with cell-secreted factors, is collected and used in the culture of a second cell

population. This is considered unidirectional communication because the second cell population cannot respond to the secreted factors and communicate back to the first population. Tissue function and disease progression often relies on bidirectional cellular communication or feedback interactions[13,16] so conditioned media transfer cannot provide a complete picture of the crosstalk that occurs *in vivo*. In addition, the soluble factors are greatly diluted and their concentration gradients are lost in the transfer. Some factors are only effective at high concentrations[9] or exhibit unique effects when experienced in a gradient.[29]

A simple method that permits bidirectional signaling and preserves soluble factor gradients is porous membrane insert co-culture. In this system, one population is cultured in the bottom of a well and another population is cultured on a porous membrane suspended 1mm above it. The populations do not touch each other, but are able to exchange paracrine signals across the porous membrane. Because the cells are separated by a distance equivalent to many cell lengths, it is possible that some short-range factors may not be able to effect their targets as they would *in vivo* and so porous membrane insert culture may not be sensitive to all types of paracrine communication.[16]

Microfabricated Reconfigurable Culture

For a more complete investigation of paracrine signaling, the co-culture technique must preserve both short-range and long-range communication. It should also allow co-culture to be rapidly initiated and discontinued so that the length of co-culture can be acutely controlled and enable very brief co-cultures (3hr or less). The method should permit easy separation of the cell populations following co-culture, as well, so that population specific responses to communication can be independently assayed.

Micromechanical reconfigurable culture[13] satisfies all of these criteria (Fig. I). In this system, cell populations are adhered to the surface of two separate comb-shaped silicon plates (combs) and co-cultured by sliding the combs together. By tightly interlocking the combs such that the edges of the finger-shaped regions contact (contact

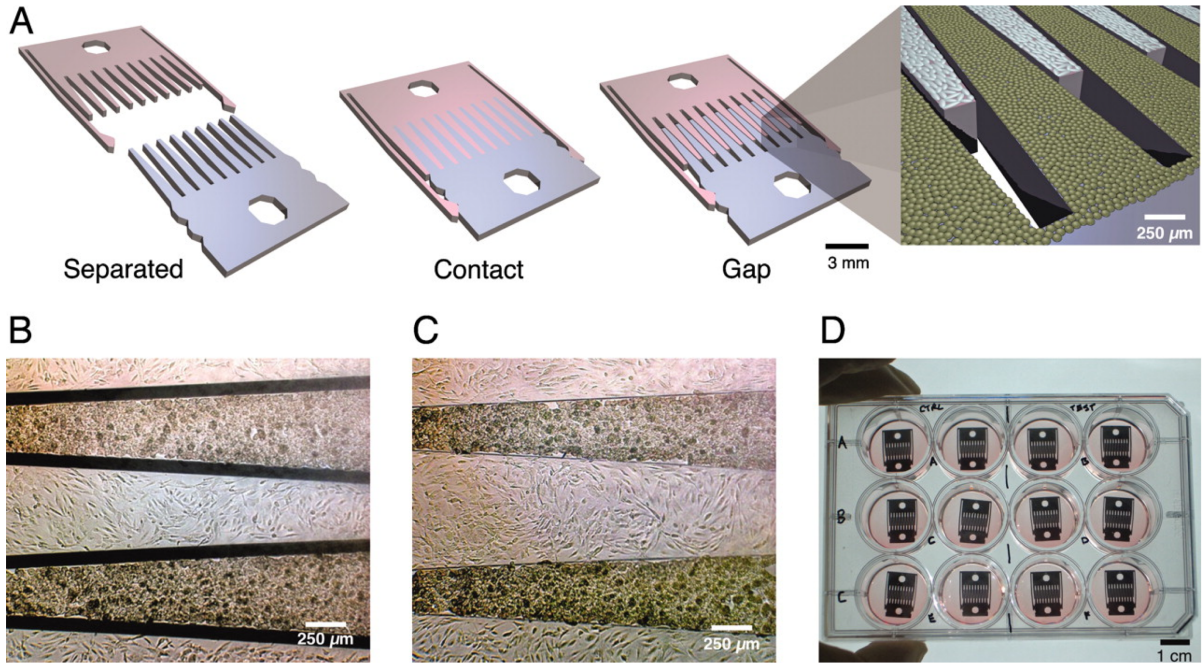

Figure I. Micromechanical reconfigurable culture. (A) Silicon comb shaped platforms can remain separated (Left), interlocked so that they achieve contact along the interface (Center), or can be interlocked with an 80-micron gap separating the two pieces (Right). Cells are cultured on the top surface of each comb piece (inset of A, and B and C) and the two populations can exchange (B) paracrine communication or (C) both paracrine and juxtacrine communication depending on configuration used. (Hui et al., 2007). Reproduced with permission from The Proceedings of the National Academy of Science.

mode, Fig. IA,C) the cell populations can exchange contact-dependent communication along the interface as well as participate in paracrine signaling. Interlocking the comb pieces such that there is an 80-micron gap separating them (gap mode, Fig. IA,B) segregates the populations so that they only undergo paracrine signaling and do not mix. Because the gap is only on the order of a few cell lengths, however, this culture method may preserve more

short-range interactions than other methods that separate the cells by a greater distance (e.g. conditioned media transfer, porous membrane inserts, and microfluidic co-culture[25]).

The comb pieces can be easily and quickly manipulated to start and end co-culture using tweezers and, following co-culture, the cell populations can be separately isolated for subsequent population-specific analysis. Easy actuation of the combs also allows for dynamic co-cultures, in which a target cell population can be serially exposed to different effector populations and different forms of cellular crosstalk (programs of both contact and paracrine communication). The plates are self-aligned and snuggly interlock using a system of V-shaped latches and matching notches. By changing the location of the notches or by adding of more of them, the spacing between the combs in the gap configuration can be adjusted to suit the needs of different studies.

The combs are microfabricated from silicon wafers using photolithography followed by deep reactive ion etching. The surface of the combs are coated with a thin layer of polystyrene using a spin coater, which is then plasma treated to mimic tissue culture plastic. ECM proteins can be adsorbed to the surface to enhance cell adhesion and viability. The devices can be reused indefinitely by removing their polystyrene coating, applying new plasma-treated polystyrene, and sterilizing them with 70% ethanol.

Previous Applications of Comb Co-culture

The versatility and unique advantages of micromechanical reconfigurable co-culture, or comb co-culture, were first exploited to investigate interactions between hepatocytes and stromal fibroblasts.[13,30,31] It was previously shown that primary hepatocytes remain viable and maintain liver-specific function *in vitro* when co-cultured with supportive mesechymal cells, but lose these abilities in their absence.[12] The comb

platform was used to determine the specific pattern of communication that is required for the maintenance of liver-specific function in the form of albumin secretion. Primary rat hepatocytes were co-cultured in the contact or gap configurations for 2 weeks with Swiss 3T3 murine fibroblasts on adjacent combs or cultured alone. Only contact co-culture was able to maintain albumin secretion throughout the entire 2 weeks. Close-range, paracrine communication from gap co-culture was not sufficient to prevent the decline of hepatocyte function. Next, hepatocytes and fibroblasts were co-cultured in contact mode for 18hr, and then the combs were separated to gap mode to continue culture for the rest of the 2-week period. Alternatively, the fibroblast comb was completely removed from culture after 18hr contact culture and hepatocytes were only exposed to fibroblast conditioned media. The transient contact followed by paracrine signaling in the gap co-culture was just as effective at supporting albumin secretion, while the complete removal of the fibroblasts after transient contact, even when conditioned media was added, resulted in the loss of function. Furthermore, when naïve fibroblasts were swapped in following transient contact, and co-cultured in gap with hepatocytes, liver-specific function was similarly maintained. This suggested that brief contact-dependent interactions with stromal fibroblasts followed by sustained close-range paracrine communication is sufficient to preserve hepatocyte function, however, reciprocal communication between hepatocytes and fibroblasts may not be necessary. After assessing hepatocyte viability in transient contact followed by gap co-culture using microscopy, it was observed that hepatocytes only survived within approximately 325μm of the tips of the fibroblast comb. A finite element model indicated that this effect could be caused by a short-range soluble factor.

These studies, which were enabled by the various unique features of comb co-culture, were very simple, yet extraordinarily informative. The co-culture system was sensitive enough to capture short-range hepatocyte-fibroblast communication because it permitted robust spatial patterning of cell populations with micrometer precision. It also helped to show that hepatocyte function could be maintained via a specific sequence of hepatocyte-fibroblast dialogue because it made it easy to rapidly manipulate within or purify entire cell populations from co-culture.

More recently, the same capabilities of comb co-culture have been utilized to study cell-cell interactions between myoblasts and fibroblasts. The differentiation of myoblasts into myotubes is crucial to muscle formation and regeneration and comb culture was used to investigate the effect of fibroblasts in the muscle environment on myoblast differentiation. We found that only contact-dependent communication with fibroblasts increased myoblast cell alignment, a desirable phenotype for myotube formation, but that cross-talk with fibroblasts in general inhibited the expression of myosin heavy chain, a marker for myoblast differentiation, and that both of these effects were mediated by FGF2.[14] Thus, this comb study showed that nearby fibroblasts may regulate muscle formation, but that additional signals are needed to achieve complete myoblast differentiation.

In addition, we modified the surface of the combs by covalently linking hydrogel of a desired stiffness to study the synergistic effects of mechanical and cellular cues on adipose derived stem cell (ASC) differentiation.[15] Specifically, we found that subjecting ASCs to both myoblast communication and culture on a substrate with a stiffness of 10kPa, each of

which has separately been shown to promote ASC myogenesis, induced significantly higher expression of myogenesis markers in ASCs compared to each alone.[15]

In this current work combs were adapted to create several new research tools including an experimental model of border formation in the developing telencephalon, a culture platform for mouse embryonic stem cells that allows for easy removal of feeder cells, and a screening platform for short-range paracrine interactions. In doing so, we were able to study interactions between populations of telencephalon progenitor cells, mouse embryonic stem cells and fibroblasts, and tumor cells and fibroblasts and to make valuable discoveries in each of these systems.

CHAPTER 1

Investigation of BMP-FGF Interactions

1.1 Abstract

Tissue complexity arises from the interaction of morphogen gradients during development. Sharp borders can be formed in contexts where morphogens that mutually inhibit one another are present in opposing gradients. One example of such an event is cortical-dorsal midline border formation in the developing telencephalon, which requires cross-inhibitory interactions of BMP and FGF signaling. It is difficult to visualize and perturb these gradients *in vivo*, so studying them *in vitro* is an attractive option. Conventional tools and culture methods, however, have not successfully been used to recreate the cortical-dorsal midline border *in vitro*. Because the comb platform compartmentalizes co-cultured cell populations, yet allows them to be rapidly manipulated into and out of co-culture, we were able to recapitulate this border *in vitro* and thus developed an experimental model for the study of BMP and FGF-dependent border formation in brain development. The versatility of the comb platform also allowed us to begin studying the effects of BMP and FGF on cortical precursor cell reorganization and migration.

1.2 Introduction

During development, interactions between gradients of opposing morphogens often trigger border formation, which ultimately allows tissues to acquire structural and functional complexity. Much attention has been devoted to discovering how cells process this information and form very sharp borders in response to it, but because of the shear

number of different morphogens and ways they interact, still more investigation is necessary to understand this phenomenon.

One such border forms during brain development. As the dorsal telencephalon differentiates, it gives rise to both the cerebral cortex and to the dorsal midline and a border is formed separating the two structures.[29] Recent findings suggest that FGFs produced by the cortex and BMPs secreted by the dorsal midline as they develop mutually inhibit signaling by each other. Cells from the developing telencephalon (dCPC) exhibited muted or speckled BMP signaling when exposed to similar concentrations of FGF and BMP compared to exposure to high BMP and low FGF concentrations.[32] Additional studies support the theory that the sharp border between the cortex and dorsal midline is created as the opposing BMP and FGF gradients mutually inhibit each other. The formation of BMP signaling borders was observed in coronal sections and inhibiting FGF signaling made the border wider and more diffuse, whereas explanted tissue cultured in FGF8 possessed an even thinner border.[33]

Greater understanding of BMP-FGF cross-inhibition and its role in forming the cortex-dorsal midline border can be achieved by recapitulating border formation *in vitro* and perturbing the morphogen gradients and receptor signaling, however this is difficult to do using conventional culture methods. The comb system allows cell populations to be rapidly patterned with micrometer-scale precision, which enables morphogens gradients to be easily generated and controlled and provides a platform in which to easily study cell migration. Thus, we used comb co-culture to recreate a border of BMP signaling in dissociated cortical progenitor cells (dCPCs) *in vitro* to serve as a model for investigating

BMP-FGF interactions in brain development. We also developed a platform to help determine how BMP and FGF affect dCPC migration and reorganization.

1.3 Materials and Methods

Comb Preparation

Combs were fabricated by photolithography and deep reactive-ion etching in the Integrated Nanosystems Research Facility at the University of California, Irvine as described.[13] The device surface was modified to resemble tissue culture plastic by spin-coating with polystyrene followed by plasma treatment. Combs were sterilized before use in 70% ethanol. After use, the devices were treated in 10% bleach, and cleaned with toluene followed by Nanostrip (Cyantek). The devices were then recoated in polystyrene and plasma-treated before the next use.

Cell Culture and Border Formation Model Preparation

CCD-18CO colon fibroblasts were obtained from ATCC (Manassas, VA), cultured in Gibco RPMI (LifeTechnologies, Grand Island, NY) supplemented with 10% Gibco FBS (LifeTechnologies) and 1% Penicillin-Streptomycin (Genesee), seeded (3×10^5) overnight onto combs in wells of a 12-well plate and used immediately in co-cultures or allowed to reach confluency in fresh media for 3 days before the start of co-culture (More Fibroblasts condition). Primary dissociated cortical precursor cells expressing the BRE-gal reporter for BMP signaling[33] or wild type cells were isolated as previously described[32] and immediately seeded (1×10^6) onto combs in dCPC culture media (DMEM with B27, N2, Na pyruvate, glutamine (GIBCO) and 1mM N-acetyl-cysteine (Sigma)) for 24hr. For migration experiments, DiO or DiI (LifeTechnologies) was added during seeding to fluorescently label the cells and BMP was added to certain wells to pretreat the appropriate cells. Excess dye

and morphogen was removed by dipping the combs in PBS twice before co-culturing the cells in new dCPC culture media for 48hr. To recapitulate border formation *in vitro*, fibroblasts and dCPCs were co-cultured in gap mode in new wells and new dCPC culture media containing 64 ng/ml BMP4 (R&D Systems, Minneapolis, MN) for 48hr. For Xgal staining (described previously[34]), combs were fixed with 4% paraformaldehyde supplemented with 2mM $MgCl_2$ and 5mM EGTA for 30 to 60min and stained for 1hr at room temperature in the dark. Combs were stained for MSX1 and with Hoechst as described.[29] Combs were imaged using an upright Olympus U-TVO.63XC microscope. Xgal-stained combs, in particular, were imaged using the 5x objective and a series of 15 images were taken across the comb surface so that staining on the entire comb could be visualized.

Image Processing

The series of images of Xgal-stained combs were stitched together to create one large image of the comb surface and the location of stained cells was recorded using the Spot Detector feature of Icy imaging software.[35] The coordinates of each stained cell was incorporated into a scatter plot using MATLAB and markers for each cell were color-coded based on the density of neighboring cells around them.

1.4 Results and Discussion

To recreate a sharp border of BMP signaling *in vitro* using combs, primary dCPCs expressing a BRE-gal reporter for BMP activity were co-cultured with 18CO fibroblasts, which naturally express FGF, in dCPC culture media containing BMP for 48hrs (Fig. 1.1).

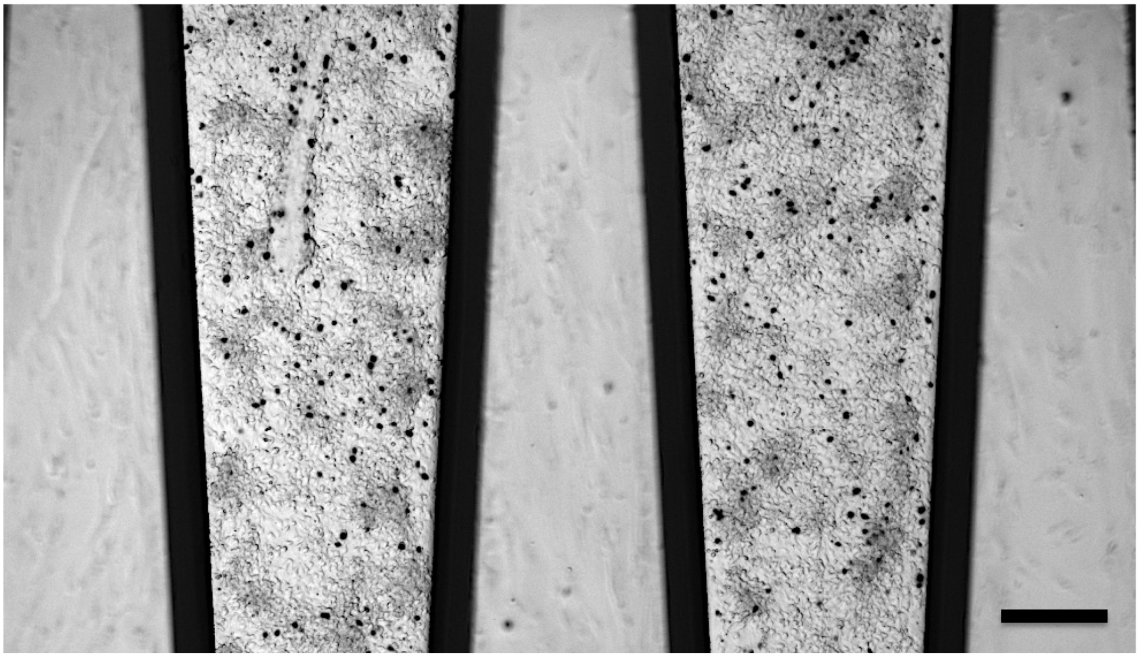

Figure 1.1 dCPCs co-cultured with fibroblasts. BRE-gal dCPCs (rounded cells on comb fingers pointing down) were co-cultured with fibroblasts (faint, elongated cells on comb fingers pointing up) for 48hr. Active BMP signaling through Xgal staining is indicated by dark coloration of cells. Because homozygous BRE-gal embryos are non-viable, heterozygous BRE-gal-WT embryos must be used instead and thus staining is not dense because not all of the dCPCs express the reporter system. Scale bar is 250μm.

Because the fibroblasts continually express FGF, an FGF gradient developed stretching from the fibroblast comb to the dCPCs. Using Xgal staining for BRE-gal reporter-induced LacZ expression, the location of dCPCs exhibiting active BMP signaling could be observed and recorded. Cortical progenitor cells with active BMP signaling were uniformly distributed along the length of the comb when they were co-cultured with dCPCs lacking the BRE-gal reporter on the adjacent comb (Control, Fig. 1.2). Yet, BMP reporter staining was not uniformly distributed along the length of the comb in dCPCs co-cultured with FGF-

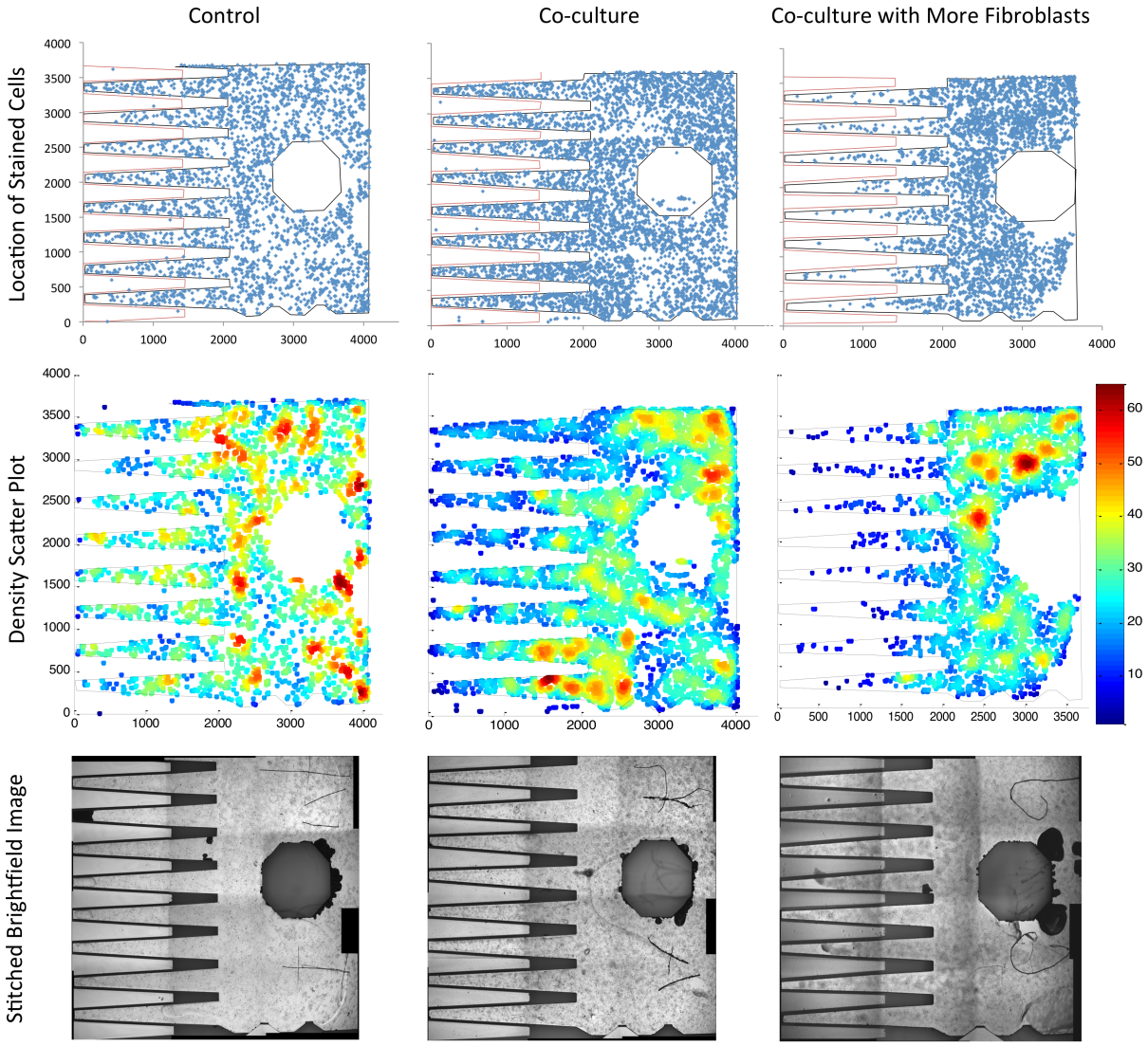

Figure 1.2. Density scatter plots of BMP signaling activation. Brightfield images of Xgal-stained dCPCs were first taken and stitched together, then the location of cells with active BMP signaling (dark cells) was recorded and used to generate a scatter plot color-coded to indicate local staining density. BRE-gal dCPCs were cultured with wild type dCPCs in the control condition, with fibroblasts in the co-culture condition, or with more fibroblasts. Color scale represents relative density.

expressing fibroblasts. As revealed by color coded density plots of stained dCPCs, staining was less dense among dCPCs on the tips of the comb fingers or, in other words, closest to the fibroblasts and closer to a higher concentration of FGF (Fig. 1.2). More strikingly, increasing the number of fibroblasts on the adjacent comb resulted in a sharp border of

BMP signaling dCPCs halfway up the comb fingers (Fig. 1.2). Very few of the dCPCs closest to the FGF gradient on the tips of the comb fingers were stained by Xgal, but staining density dramatically increased starting from the middle of the comb fingers and progressing toward the back of the dCPC comb. Upon closer observation, the border appeared to form just past the tips of the comb containing fibroblasts. These results show that we were able to generate a border of BMP signaling *in vitro* using precisely patterned fibroblasts to provide the FGF gradient necessary to inhibit BMP signaling up to a threshold distance away from the fibroblast comb.

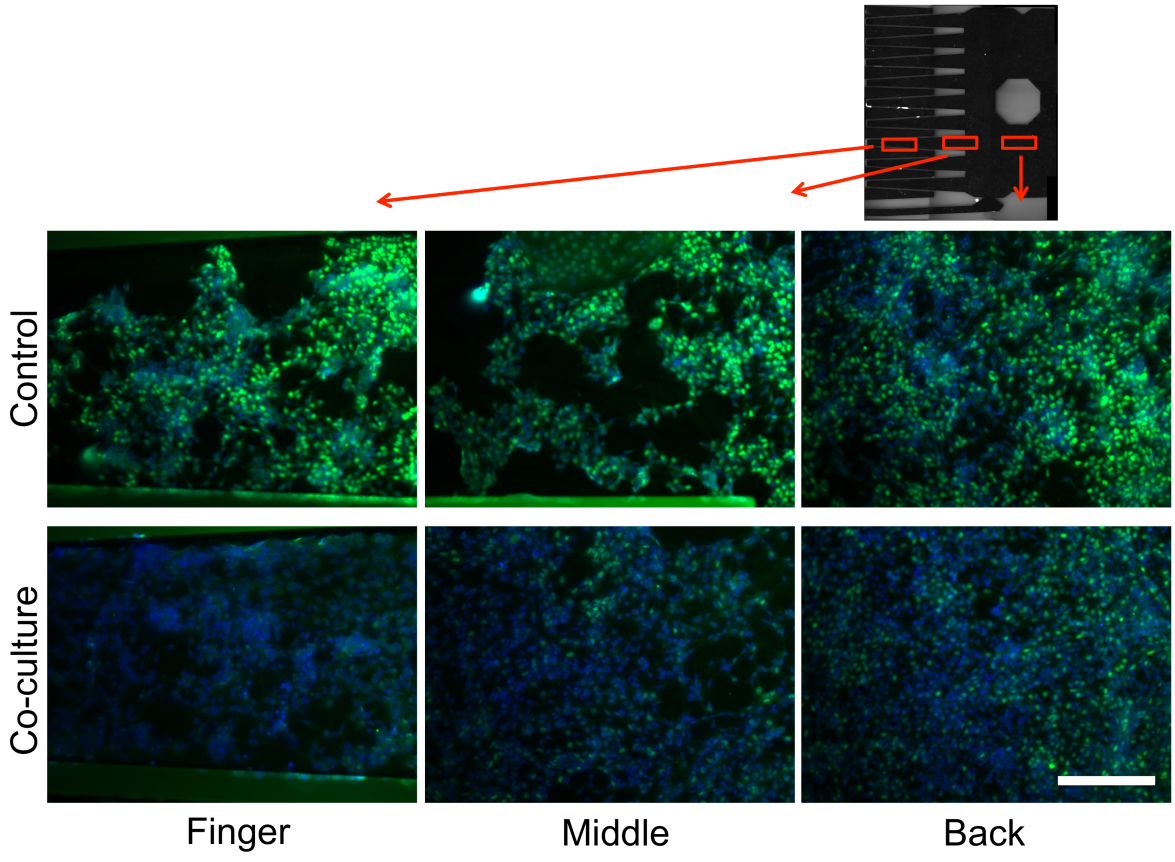

Figure 1.3. MSX1 expression verifies that the culture conditions induce BMP signaling border formation. Wild type dCPCs from control culture and fibroblast co-culture were stained for the expression of BMP target gene MSX1 (green) and counterstained with Hoechst (blue). Representative images from the fingers, middle of the comb, and the back of the comb are shown. Scale bar is 250μm.

To verify that BMP signaling was truly being inhibited by the fibroblast-derived FGF gradient, co-cultured dCPCs were stained to measure the expression of a BMP pathway target gene, MSX1. MSX1 immunofluorescent staining was more faint and diffuse in dCPCs on the fingertips, but brighter in cells midway along the length of the comb and on the back of the comb (Co-culture, Fig. 1.3). By comparison, dCPCs cultured with dCPCs on the adjacent comb were uniformly bright along the length of the comb and even exhibited a much higher fluorescent signal than the brightest dCPCs in the co-culture. It is likely that the dCPCs that were farthest away from the fibroblasts in co-culture still experienced enough FGF to inhibit BMP pathway activation and reduce the intensity of MSX1 staining slightly. Thus, results of MSX1 staining verify that we successfully recreated BMP signaling border formation *in vitro* by co-culturing dCPCs and FGF-producing fibroblasts on combs in media containing BMP.

Now that we have developed an *in vitro* model of border formation in the developing telencephalon that incorporates BMP-FGF cross-inhibition, we can perturb the system to gain a deeper understanding of the mechanisms mediating this event. The FGF gradient can be altered by adding more or fewer fibroblasts or by overlaying the comb co-culture with collagen gels of different densities to prevent vertical diffusion of FGF into the culture media. FGF and BMP signaling can be perturbed by using the pan-FGF receptor inhibitor PD173074, adding different concentrations of BMP, or replacing the FGF gradient with a BMP gradient by substituting a cell line that expresses BMP. The slope and strength of the morphogen gradients can be measured by fluorescently staining the morphogens in the cultures or by using a cell line that produces FGF or BMP fused with GFP. In doing so

and comparing this to the location of the border, the threshold concentration of FGF that inhibits BMP signaling can be determined.

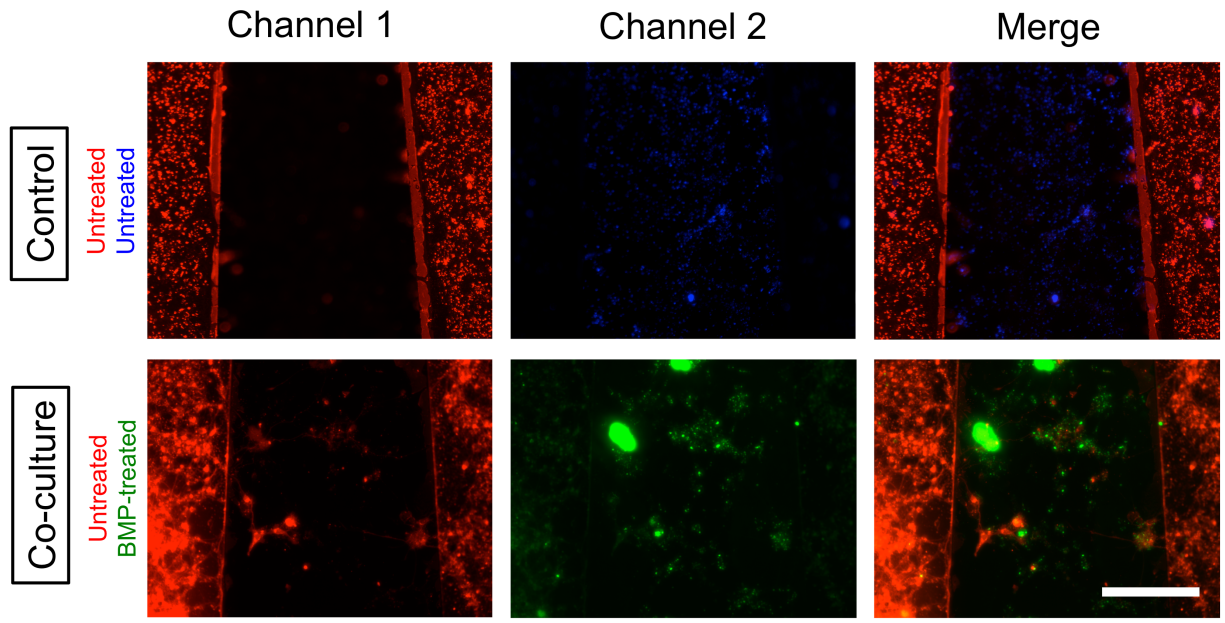

Figure 1.4. BMP treatment induces dCPC migration and neuronal morphology. Fluorescently-labeled wild type dCPCs (red) were co-cultured in the contact mode with other wild type cells (blue) (Control) or with BMP-treated dCPCs (green). After 48hr, untreated dCPCs migrated onto the comb containing BMP-treated cells and cells on both combs adopted a more spindle-like appearance resembling neurons. Scale bar is 250μm.

Finally, the comb platform was used to begin to study the effect of BMP and FGF signaling on dCPC migration. When untreated dCPCs were co-cultured with dCPCs pre-treated with BMP, both types of cells appeared to adopt a neuronal morphology and untreated cells migrated onto the comb containing BMP-treated cells (co-culture, Fig. 1.4). In contrast, untreated dCPCs cultured with untreated dCPCs on the adjacent comb maintained a spherical morphology and did not migrate (control, Fig. 1.4). These findings are supported by studies suggesting that BMP can induce neurogenesis and can regulate neural progenitor cell migration.[36]

In summary, we have developed a model of border formation in the developing brain and have adapted comb co-culture to study progenitor cell migration in response to various morphogens. These platforms can be valuable tools for investigating BMP and FGF-mediated migration and border formation, however, they can easily be adapted to study other morphogen gradient systems involving factors such as Hedgehog (HH) and Decapentaplegic (Dpp). Thus, the work described in this chapter has wide-spread applications.

1.5 Acknowledgements

This work was performed with the help of co-authors Ernest S. Fung, Elliot E. Hui, and Edwin S. Monuki and was supported by Chao Family Comprehensive Cancer Center through NCI Center Grant (P30A062203) and the American Cancer Society (ACS/IRG 98-279-07). K.H.S was supported by fellowships from the NSF (GRFP) and the NIH (T32-HD060555).

CHAPTER 2

A New Method of Mouse Embryonic Stem Cell Culture and Investigation of mESC-Feeder Cell Interactions

2.1 Abstract

Mouse embryonic stem cells (mESCs) are traditionally grown on a feeder layer of mitotically inactive mouse embryonic fibroblasts to provide a culture environment that promotes proliferation and inhibits differentiation of the pluripotent stem cells. Often, it later becomes important to remove the feeder cells from the stem cells, for example to avoid confounding effects when assaying stem cell gene expression. However, standard methods used to remove feeder cells from mESC cultures can be incomplete and/or inefficient. Here we co-culture feeder-dependent mESCs and feeder cells on combs in the gap configuration and show that the close proximity of gap culture is sufficient to maintain stem cell characteristics similar to the conventional culture method, while Transwell and conditioned media culture do not maintain them. In addition, we demonstrate how gap comb co-culture allows for simple extraction of mESCs to yield stem cell samples that are virtually free of feeder cells.

2.2 Introduction

Mouse embryonic stem cells (mESCs) are derived from the inner cell mass (ICM) of blastocyst embryos.[37,38] To establish mESCs, the blastocyst or isolated inner cell mass is typically placed on a monolayer of mitotically inactivated mouse embryonic fibroblast cells known as a feeder layer. The feeder layer helps provide conditions that promote proliferation and suppress differentiation of pluripotent cells.[39] Although some mESC lines

were established or adapted to culture in the absence of feeders, many mESC lines are feeder-dependent and still routinely grown on feeder layers. When cultured in the absence of feeders, feeder-dependent mESC lines often differentiate even when growth factors and medium conditioned by feeders are present. In contrast to mouse ESCs, human ESCs have different growth factor requirements, are more easily adapted to feeder-free culture conditions, and are thought to represent pluripotent cells of a slightly later development stage than mESCs.[40]

When studying mESCs it is often necessary to perform gene or protein expression assays that require populations that are free of contaminating feeder cells, but that can be problematic to achieve. Two techniques are commonly used to remove the feeders, preplating and gradient centrifugation.[41] In the preplating method, feeder and mESC separation depends on the fact that feeders adhere to tissue culture dishes more quickly than mESCs. In the gradient centrifugation method, mESCs and feeders are separated by size using centrifugation in a concentration gradient of polysucrose and sodium diatrizoate (Histopaque). Both methods can leave behind feeder cells in the mESC fraction and can result in significant loss of mESCs from the sample.

In this work the mESCs and feeders were separately seeded onto the fingers of individual combs, and comb pairs were then locked together with a separation of 80 μm between opposing fingers. This distance was sufficient to prevent movement of the feeders to the mESC compartment. After culture, the stem cells were easily and cleanly harvested by physically separating the compartment containing stem cells from that containing the feeders. Our method yielded mESC samples with substantially fewer contaminating feeder cells than the conventional preplating method and virtually no loss of mESCs. In contrast,

both the preplating and gradient centrifugation methods resulted in a substantial loss of mESCs.

Mouse ESCs cultured using this method formed colonies of cells that were morphologically similar to mESCs grown with feeders in tissue culture dishes. In contrast, morphological changes consistent with differentiation were observed in mESCs grown without feeders. Further, mESCs cultured using this method expressed Oct4, a transcription factor expressed by pluripotent stem cells, in quantities comparable to that of mESCs grown with feeders and significantly higher than that of mESCs cultured in parallel without added feeders, feeder conditioned media, or feeders in Transwell culture. This indicates that close proximity gap comb co-culture may prevent mESC differentiation just as effectively as feeder-layer culture and better than methods in which the feeder cells are farther away from mESCs or absent. Thus, our technique is useful for culturing feeder-dependent mESCs in situations that require efficient removal of feeder cells while retaining pluripotent stem cell characteristics. It also demonstrates how useful features of gap comb co-culture, like close-proximity and easy purification of populations, can be for manipulating and studying cells.

2.3 Materials and Methods

Comb Gap Measurement

Brightfield reflected light images of pairs of combs in the gap configuration and of a microscope scale slide were obtained using an upright Olympus U-TVO.63XC microscope. The actual measurement of the gap distance was determined by converting the pixel length of the gap (acquired in ImageJ (National Institutes of Health)) to microns using the microscope scale slide.

Cell Culture on Tissue Culture Plates

GSI-1 mESCs were cultured in DMEM with 16% FBS (Omega Scientific), HEPES, L-glutamine, non-essential amino acids, penicillin/streptomycin, and β-mercaptoethanol (Sigma). All reagents were acquired from LifeTechnologies, unless otherwise noted. Leukemia inhibitory factor (LIF, Millipore) was added at 1000 units/mL. Mitomycin-c treated MEF feeders (Millipore) were plated in DMEM with 10% FBS, non-essential amino acids, L-glutamine, and penicillin/streptomycin at density of 105,000 cells per well of a 12-well plate precoated with 0.1% gelatin (Sigma). mESCs were plated at a density of 175,000 cells per well of a 12-well tissue culture plate. To prepare conditioned medium, mECS medium in which feeders had been cultured for 24hr was diluted with fresh mECS medium 2 to 1 and LIF was added at 1000 units/mL.

Cell Culture on Comb Substrates

mESCs from a standard feeder layer culture were seeded onto two gelatin-coated male combs in a well of a 12-well plate at a density of 250,000 cells in 1ml of medium. In a separate well, feeders (500,000 cells in 1 ml of medium) were seeded onto gelatin-coated female combs. After 5 hours, each mESC comb was interlocked with a feeder comb, with the opposing fingers either in direct contact or separated by a gap. Cells were cultured for 2 days with the medium changed daily. To collect the mESCs for analysis, the feeder comb was removed and the mESCs on the fingers of the mESC comb were collected using a cell scraper.

Migration Assay

Feeder cell migration between adjacent combs was assayed by staining the feeders with DiI (Molecular Probes) for 20 minutes prior to seeding. Cells were seeded on a

gelatin-coated comb. After 5 hours, the comb was interlocked with a gelatin-coated comb without cells, with the opposing fingers either in direct contact or separated by a gap. The cells were then cultured for 2 days. Fluorescent and brightfield reflected light images were obtained using an upright Olympus U-TVO.63XC microscope.

Feeder Removal by Preplating

mESCs cultured on feeders were trypsinized and resuspended in mESC medium to 1 x 10^6 cells per ml. 250 µl of the cell suspension was plated onto a gelatin-coated well of a 12-well tissue culture plate and incubated at 37˚C, 5% CO_2 for 20 minutes, and the cell suspension was then collected and transferred to a fresh gelatin-coated dish. After 20 minutes at 37˚C, 5% CO_2, the cell suspension was collected and centrifuged at 1500xG for 3 minutes. The cell pellet was resuspended in mESC medium. The cells were counted prior to and after preplating using a hemocytometer. The feeders, distinguished by size, were not included in the cell count. All cell counts were performed in triplicate.

Feeder Removal by Gradient Centrifugation

The concentration gradient was prepared in a glass test tube with Histopaque-1119 (Sigma) diluted in DMEM, as previously described.[41] Briefly, the gradient was layered in the tube, from bottom to top, as follows: 1ml 100%, 1ml 60%, 0.5ml 40%, and 0.5ml 20%. mESCs grown on feeders were trypsinized and resuspended in mESC medium to a density of 1 x 10^6 cells per ml. 250µl of the cell suspension was slowly pipetted on top of the gradient and the tube was centrifuged for 13 minutes at 400xG. After centrifugation, the mESCs were found at the interface of the 60% and 100% Histopaque-1119 solutions, whereas the feeders were at the 20% and 40% interface. The mESCs were collected from

the upper layers of the gradient. The cells were washed in DMEM three times and resuspended in mESC medium. The cells were counted as described above.

Flow Cytometry

Cells from the fingers of 5 combs or 1 well of a 12-well plate were trypsinized and resuspended in PBS, then fixed in 4% paraformaldehyde for 10 minutes on ice. An equal volume of 0.1% Triton X-100 was added for permeabilization and incubated for 10 minutes on ice. Cells were washed twice in PBS, resuspended in FSP-1 antibody (Millipore) in 1% donkey serum (LifeTechnologies), and incubated for 30 minutes on ice. Cells were washed twice, resuspended in donkey anti-rabbit 647 secondary antibody (LifeTechnologies) in 1% donkey serum, incubated for 15 minutes on ice, washed twice in PBS, and resuspended in PBS. The cells were analyzed using a BD LSRII flow cytometer and the data were analyzed using FloJo Software. All conditions were tested in triplicate.

Immunocytochemistry

Cells were fixed in 4% paraformaldehyde, permeabilized with 0.1% Triton X-100, blocked in 10% donkey serum (LifeTechnologies), incubated in Oct4 antibody (Santa Cruz N-19) in 1% donkey serum, washed, and incubated donkey anti-goat 488 antibody (LifeTechnologies). Hoechst 33342 (LifeTechnologies) was used to visualize the nuclei. Images were obtained using a Nikon TI inverted microscope.

qRT-PCR

RNA was extracted using the PureLink Midi RNA Extraction Kit (LifeTechnologies) and cDNA prepared using the SuperScript III Reverse Transcription Kit (LifeTechnologies). Cells from 4 combs or one well of a 12-well plate were used for RNA extraction. Real time PCR was performed using the ABI ViiA7 Sequence Detection System, with the Taqman

Universal Master Mix and the following primer/probe assays: Oct4 Mm00658129_gH and Fsp1 Mm00803372_g1. β-Actin was used as the endogenous control (ABI). Samples were analyzed in triplicate for each of three biological samples for each gene. Data was analyzed with ViiA7 RUO software (Life Technologies) using the 2ΔΔct method. Expression levels for each probe were normalized to the levels of β-actin.

2.4 Results

The goal of this study was to use mESC-feeder cell interactions to determine if gap comb co-culture provides sufficient proximity between cell populations to allow for important paracrine crosstalk to occur, while still enabling pure populations to be easily and rapidly isolated from one another. Specifically, we wanted to observe whether gap comb co-culture of feeder-dependent mESCs with feeders 80 microns away rather than in direct contact through traditional feeder-layer culture could maintain stem cell markers, and yield pure populations of mESCs. Mouse ES and feeder cells were seeded onto the fingers of individual combs, and then the combs were locked together to form co-cultures (Fig. 2.1). Both mES and feeder cells adhered well to gelatin-coated combs 5 hours following seeding (data not shown). The mESCs adhered to the substrate singly or in small groups of a few cells, whereas the feeder cells formed a nearly confluent layer. Combs were positioned in contact mode, with the fingers either in direct contact (Fig. 2.1A,C,E), or in gap mode, with an 80 ± 0.7 μm gap separating the opposing fingers (Fig. 2.1B,D,F). After 2 days in co-culture, the mESCs formed colonies on the comb surface that were similar to, but slightly more flattened than, mESCs grown on feeders in tissue culture dishes coated

with gelatin (standard conditions) (Figs. 2.1A,B, 2.3A,B). The cultures were

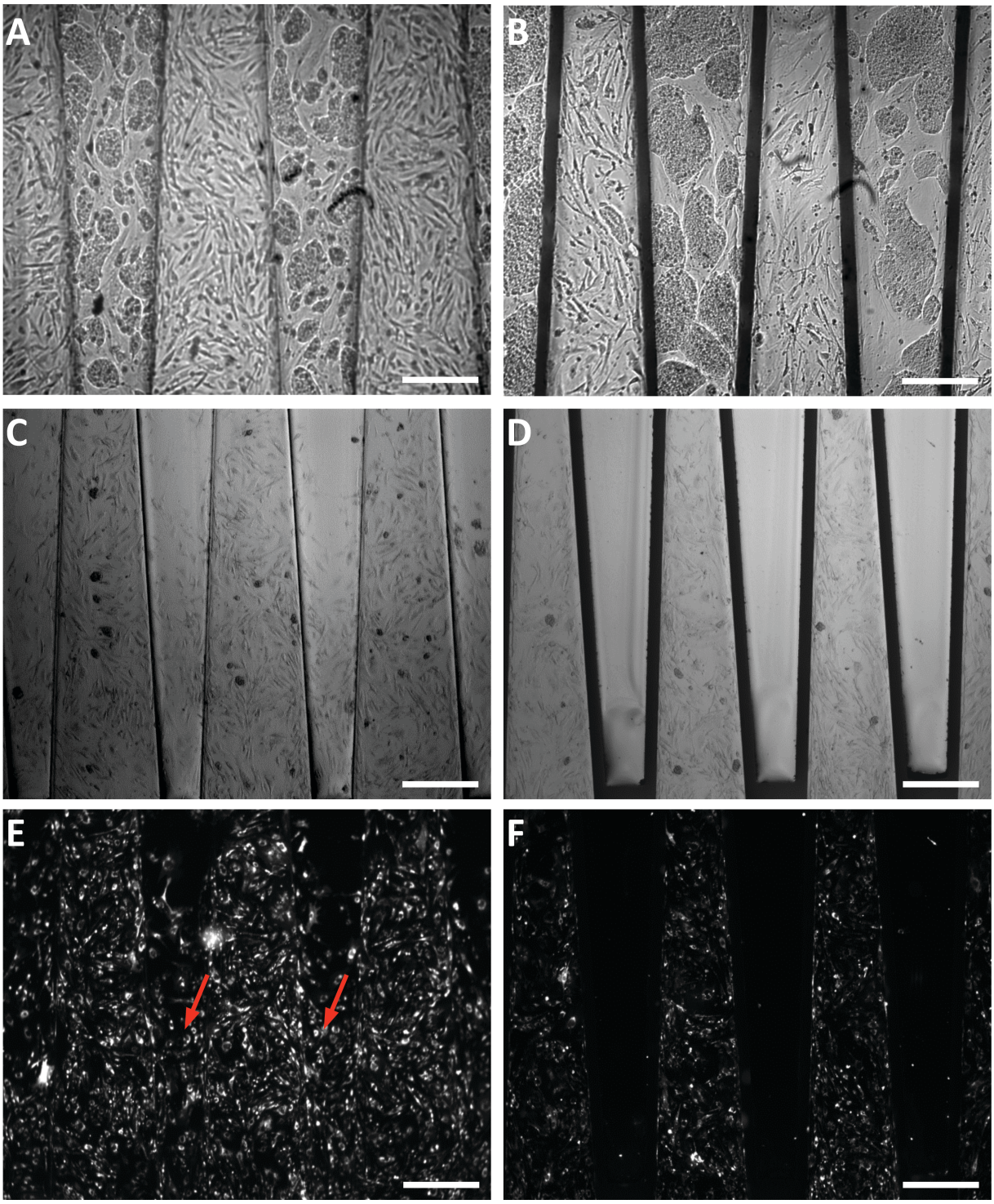

Figure 2.1. Growth of mESCs on micromechanical comb substrates. (A) Brightfield reflected light image of mESCs cultured on comb substrate in the contact mode. (B) Brightfield reflected light image of mESCs cultured on combs in the gap mode. (C,E)

Brightfield reflected light and fluorescent images of feeders prestained with DiI, cultured on a comb paired in contact mode with a comb to which no cells were added. Red arrows show feeders that have migrated onto adjacent fingers. (D,F) Brightfield reflected light and fluorescent images of feeders prestained with DiI, cultured on comb paired in gap mode with a comb to which no cells were added. Scale bars are 300 μm.

were observed by brightfield reflected imaging. As expected, few, if any, feeder cells migrated onto mESC fingers in cultures grown in gap mode, whereas many feeder cells migrated onto mESC fingers in contact mode culture (Fig. 2.1A,B). To determine the extent of the feeder cell migration more directly, feeder cells prestained with a fluorescent dye (Dil) were seeded on gelatin-coated combs then locked in gap or contact mode with gelatin-coated combs that were not seeded with cells. After 2 days in contact mode culture, many feeder cells were observed on the gelatin-coated fingers that had not been seeded with feeder cells (Fig. 2.1C,E). In the gap configuration, very few feeder cells were observed on the fingers that had not been seeded with feeder cells (Fig. 2.1D,F). Thus, we concluded that feeder cells were able to move to adjacent fingers when cultured in contact mode, but not in when cultured in gap mode.

To measure the purity of mESC populations isolated from gap comb co-culture, we determined the number of feeders remaining among the mESCs after separation and compared it to results achieved using common methods of isolating mESCs from standard feeder-layer culture, preplating and gradient centrifugation. The number of feeders remaining in purified samples was quantified by flow cytometry using Fsp1 as a fibroblast marker (Fig. 2.2A). As shown in the first two panels of Fig. 2.2A, Fsp1 expression is much lower in mESCs compared to feeders. The proportion of cells with Fsp1 expression comparable to feeders was determined in samples of mESCs from feeder-layer culture and

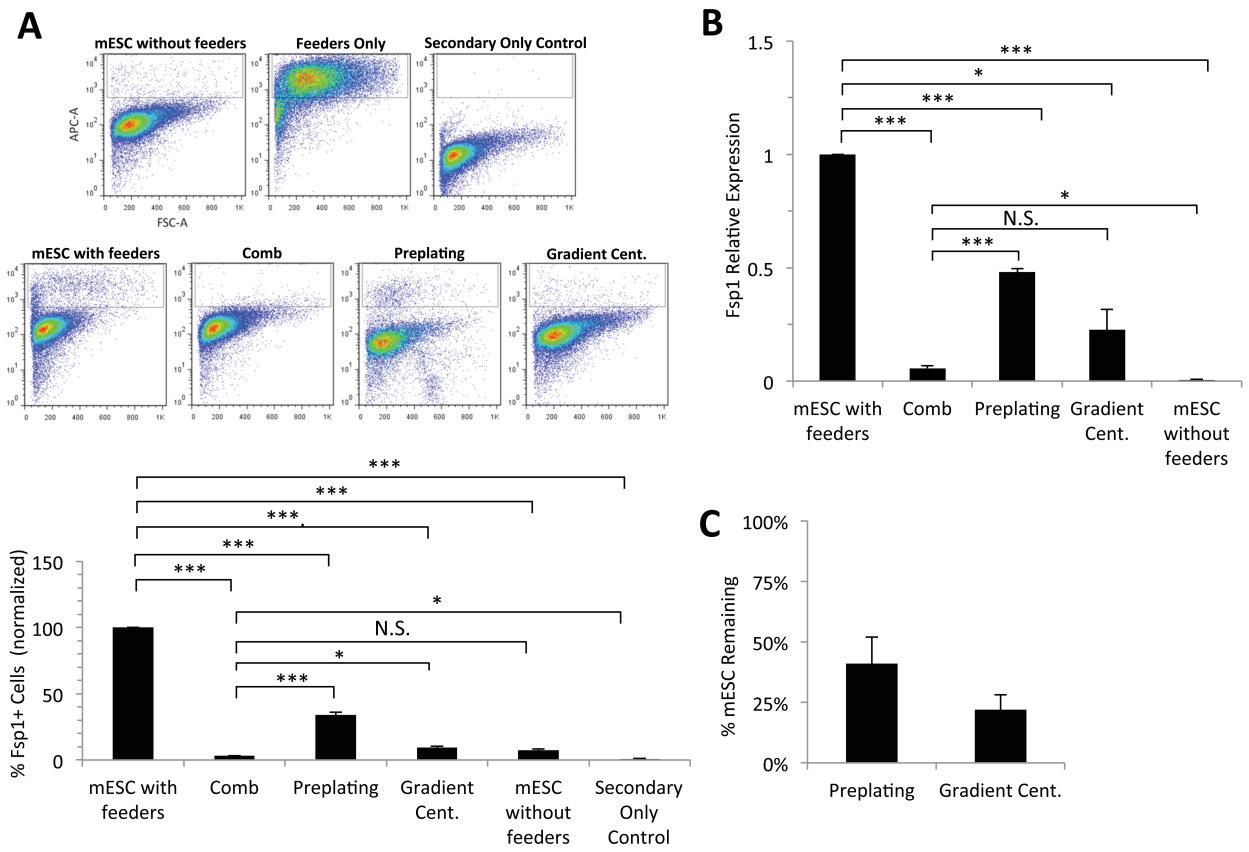

Figure 2.2. Feeder retention and mESC loss using preplating, gradient centrifugation, and comb culture methods. (A) Flow cytometric analysis of fibroblast-specific gene, Fsp1, expression in samples of mESCs cultured without feeders (mESC without feeders), feeder cells (Feeders only), mESCs cultured with feeders in standard conditions (mESC with feeders), mESCs separated from feeders after culture on combs in gap mode (Comb), mESCs separated from feeders by preplating (Preplating), mESCs separated from feeders by gradient centrifugation (Gradient Cent.), and in mESCs cultured in standard conditions without incubating with the primary antibody for Fsp1 (Secondary Only Control). Results are displayed as the percentage of the unpurified standard condition. (B) qRT-PCR analysis of Fsp1 expression in samples of unpurified mESCs cultured in standard conditions with feeders (mESC with feeders), in mESCs separated from feeders after culture on combs in gap mode (Comb), mESCs separated from feeders by preplating (Preplating), mESCs separated from feeders by gradient centrifugation (Gradient Cent.), and in mESCs cultured without feeders. Results are displayed as fold-change compared to unpurified mESC cultured with feeders. (C) Percentage of mESCs remaining after feeder removal. Cells were counted before and after removal of feeders from mESCs for both preplating and gradient centrifugation methods. For all graphs, error bars represent the standard error of the mean (n=3). Statistical analysis performed using Student's t test and "*" = $p < 0.05$ and "***" = $p < 0.005$, and N.S. denotes not significant.

used as 100% in further analyses. Samples purified by the preplating method contained 33.8% that of Fsp1+ cells present in standard cultures, whereas gradient centrifugation and our comb method reduced the Fsp1+ cells to 9.4% and 3.2%, respectively. In fact, the samples purified using the comb method retained fewer Fsp1+ cells than the mESCs plated without added feeders, 3.2% versus 7.5%. We also estimated the quantity of feeders remaining after purification using qRT-PCR (Fig. 2.2B). After separation by any of the 3 methods, Fsp1 expression was reduced relative to that of mESCs grown in standard feeder-layer culture. Fsp1 expression in samples purified using the preplating method was reduced to about half that of standard cultures. The gradient centrifugation method reduced Fsp1 expression to about a quarter that of standard cultures. Fsp1 expression was further reduced in samples purified using the comb method to a level nearly as low as mESCs grown without added feeders. Results from analysis of Fsp1 expression suggest that mESC samples purified by the comb method contained fewer contaminating feeders than those purified by preplating or gradient centrifugation methods.

Both the preplating and gradient centrifugation methods of feeder cell removal involve multiple steps in which mESCs can be lost. In contrast, with comb substrates, purification is accomplished simply by separating the feeder comb from the mESC comb and requires no additional steps. In order to determine the extent of mESC loss in preplating and gradient centrifugation methods, mESCs were counted before and after subjecting the cells to preplating or gradient centrifugation. Using the preplating method, approximately 41% of the mESCs were recovered, whereas using the gradient centrifugation method only 22% of the mESCs were recovered (Fig. 2.2C). Clearly, both preplating and gradient centrifugation methods result in large loss of mESCs during the

purification process. Such losses would be detrimental in situations in which the number of mESCs is already low. In contrast, comb separation, by design, does not incur mESC loss because no additional steps are required to remove the feeder cells from the mESCs.

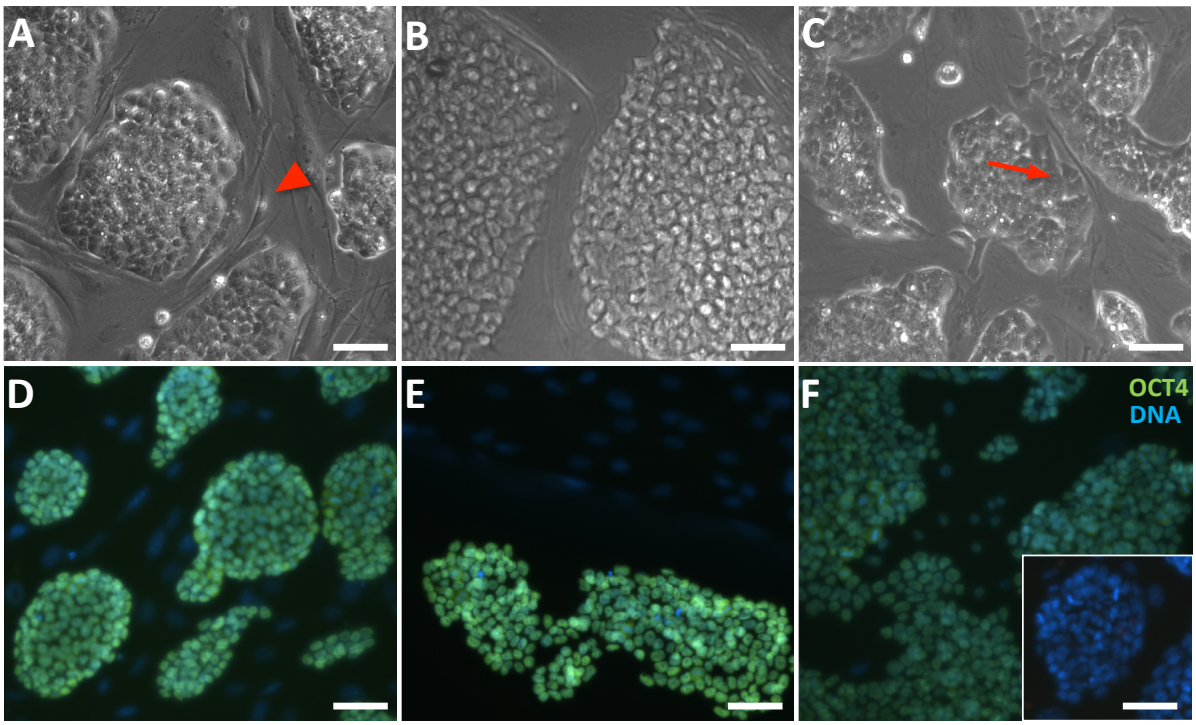

Figure 2.3. Morphology and Oct4 expression in mES cells. (A) Phase contrast image of mESCs in standard culture on a layer of mitotically inactive MEFs (feeders indicated by red arrow head), (B) brightfield reflected light image of mESC culture on a comb co-cultured in gap mode with a second comb covered with feeders, and (C) phase contrast image of mESCs cultured in the absence of feeders with a differentiating cell highlighted by red arrow. (D,E,F) Fluorescent images of Oct4 (green) and DNA (blue) in (D) standard culture of mESCs with feeders, (E) cultures of mESCs with feeders on adjacent fingers in gap mode, and (F) cultures of mESCs in the absence of feeders with secondary antibody control in inset. Scale bars are 50 μm.

Since we were able to demonstrate that gap comb co-culture permits rapid purification of populations for subsequent use, we next examined whether the distance between the populations in gap co-culture was small enough to capture sufficient cellular communication to maintain the pluripotency state of mESCs. After 2 days of gap culture

with feeders, mESC colonies were slightly flatter than those grown in standard conditions on feeders but were otherwise morphologically similar (Fig. 2.3A,B). In contrast, the mESCs cultured in the absence of feeders had cells on the edges of the colonies with altered shapes, a morphology consistent with differentiation (Fig. 2.3C). To further explore the differentiation state of the mESCs, we assayed expression of Oct4, a transcription factor that is highly expressed in pluripotent cells including mESCs.[24] Oct4 expression was visualized by immunocytochemistry. Oct4 expression was similar in gap culture and standard culture on a feeder layer (Fig. 2.3D,E). In contrast, Oct4 expression was reduced in cells cultured in the absence of feeders (Fig. 2.3F).

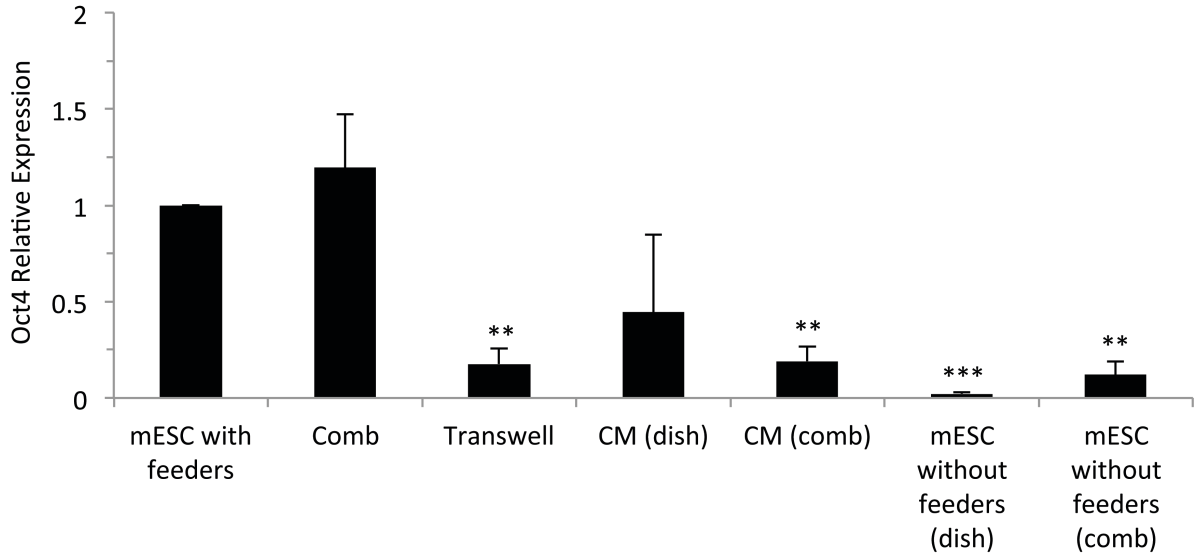

Figure 2.4. Oct4 expression in mESCs grown in various culture conditions. Oct4 expression determined by qRT-PCR in mESCs grown in standard feeder conditions (mESC with feeders), mESCs grown on combs paired with feeders on adjacent fingers in gap mode (Comb), mESCs grown on a tissue culture dish with feeders at a distance of about 1mm separated by a microporous membrane (Transwell), mESCs grown in conditioned medium without feeders on a tissue culture dish [CM (dish)], mESCs grown in conditioned medium without added feeders on a comb [CM (comb)], mESCs grown without added feeders on tissue culture dish [mESC (dish)], mESCs cultured without added feeders on a comb [mESC (comb)]. Error bars represent the standard error of the mean (n=3). Statistical analysis performed using Student's t test. "*" = $p<0.05$, "**" = $p<0.01$, "***" = $p<0.005$.

We next determined relative expression of Oct4 mRNA in the 3 culture conditions by qRT-PCR (Fig. 2.4). In comb culture, Oct4 was maintained at a quantity similar to that of mESCs grown with feeders in standard conditions (1.19 fold). In contrast, Oct4 decreased significantly when the cells were grown in the absence of feeders on either tissue culture dishes or comb substrates (0.02 fold, 0.12 fold). Oct4 also decreased when feeder-conditioned medium was added to replace the feeders either on tissue culture dishes or comb substrates (0.45 fold, 0.19 fold). Further, Oct4 decreased in mESCs grown with the feeders contained within a transwell chamber and separated by a microporous membrane (0.18 fold). These results suggest that 1. Oct4 expression is not reduced in our culture system in which the mES and feeder cells are separated by a 80 ± 0.7 μm gap, 2. Oct4 expression is reduced when feeder-dependent mESCs are cultured without feeders, and 3. the reduction cannot be mitigated completely by addition of feeder conditioned medium or feeders separated from the mESCs by a microporous membrane in a transwell

2.5 Discussion

The results presented here support two conclusions. First, highly pure samples of cells, such as feeder-dependent mESCs, can be easily isolated from gap comb co-culture without loss of the cell type of interest. Second, gap comb co-culture allows cell populations to share important close-range paracrine communication, which in this case supported pluripotency marker expression in mESCs that were previously thought to require direct contact with feeder cells.

In addition to demonstrating the utility of gap comb co-culture, this study also unveiled a new method to culture mESCs. Effective removal of feeder cells from mESC

cultures is critical for many studies including preparing mESCs for microinjection into blastocyst-stage embryos to make chimeric mice and for RNA and protein expression analysis. Contamination of mESC samples with feeder cells introduces uncertainty in the interpretation of expression data because any RNA or protein detected might be derived from contaminating feeder cells. With the comb co-culture method, cell populations can be held in close proximity but not actually combined, allowing for rapid and efficient retrieval of individual populations. Specifically, we demonstrated that mESC samples purified using the comb method contained fewer contaminating feeders and retained more mESCs than preplating or gradient centrifugation. Additionally, feeder cell contamination using our comb method is more than 5-fold lower than that observed in a recently reported microfluidic feeder-layer system that uses porous membranes to keep the mESCs and feeder cells in separate compartments.[24] The number of feeders observed in mESCs purified by our comb method was 3.2% that found in mESCs cultured with feeders in standard conditions (i.e. results were normalized to the number of feeders present in the mESC+feeders). When the results in Chen et al., 2013 are calculated in the same manner, the extent of feeder contamination is more than 5-fold higher than the feeder contamination we observed. Importantly, porous membranes not only allow cell contact through the pores but can also allow cell migration.[42] We demonstrated that very few, if any, feeder cells migrate to the mESC compartment using our comb method.

Our results suggest that preplating and gradient centrifugation result in feeder contamination and mESC loss. The advantage of the preplating method is that it is an easy and fast technique that does not require specialized reagents and can be used for large numbers of cells. Hence, preplating might remain the preferred method for situations in

which large numbers of cells are available and some contamination with feeders can be tolerated. For greater mESC purity, gradient centrifugation is more effective, but mESC loss is extensive. A drawback of gradient centrifugation is that it requires specialized reagents (e.g. Histopaque) and leaves the cells sticky, even after repeated washes. The increased stickiness of the cells makes it difficult to work with them and might affect their properties. Co-culture of mES and feeder cells on comb substrates offers the advantage of efficient feeder removal without loss of mESCs. After purchase of the manufactured comb devices, they are reusable and inexpensive to maintain. One drawback is that the combs have a small surface area, thus the number of cells that can be grown is limited. However, for growing small samples for RNA or protein extraction or microinjection, comb substrates are an effective tool for obtaining mESCs with little or no feeder contamination.

Furthermore, we show here that even though the mES and feeder cells are separated by 80 μm, the mESCs retain expression of a marker characteristic of pluripotent cells, Oct4. In contrast, Oct4 expression dropped in mESCs grown in parallel without added feeders consistent with initiation of differentiation. Differentiation was not observed when feeders were kept nearby in the gap mode. A drop in Oct4 expression was not prevented when medium conditioned by feeders was added or when ES cells were grown about 1mm away from feeders suspended in a transwell, suggesting that secreted factors that act at long range (>1 mm) are not sufficient. These observations suggest that close proximity (<1mm) of the mESCs and feeders is required to maintain mESCs. Oct4 expression was maintained when the mESCs and feeders were separated by small gap. This suggests that maintenance of mESCs does not require cell-cell contact but rather close proximity. A number of reports have demonstrated that ESCs can be grown by plating ESCs and feeders

directly on opposite sides of a porous membrane that allows direct cell-cell contact through the membrane.[42-44] Our results suggest that direct contact between the cells is not needed, but rather close proximity of the ESCs and feeders is sufficient.

Two growth factors, LIF and BMP, are known to be required to maintain mESCs.[39] In routine culture of mESCs, LIF is added to the culture medium and also produced by the feeders. LIF activates the JAK/STAT pathway. BMP, either present in the serum or added to the culture medium, is also secreted by feeders and supports mESC maintenance by inhibiting the Erk/MAPK pathway.[45] One possibility is that a high local concentration or short-lived forms of LIF and/or BMP are required that are provided by the feeders. Indeed, Bmp4 was previously reported to act as a short-range factor.[46] Alternatively, a different factor that acts at short-range could be produced by feeders and required for the maintenance of mESCs. Possible candidates include Wnt5a and Wnt6 that are produced by feeders and able to support self-renewal of mESCs.[47] The microfabricated substrate culture system described here provides an excellent platform for further study of the factors that act at short range to maintain self-renewal and/or block differentiation of mESCs.

2.6 Acknowledgements

This work performed with the help of co-authors Noelle G. Thompson, Elliot E. Hui, and Leslie F. Lock. It was supported by institutional funds from the University of California, Irvine (to L.F.L.). E.E.H. was supported by the Chao Family Comprehensive Cancer Center through NCI Center Grant (P30A062203) and the American Cancer Society (ACS/IRG 98-279-07). N.G.T. was supported by a fellowship from CIRM Training Grant (TG2-01152). K.H.S was supported by fellowships from the NSF (GRFP) and the NIH (T32-HD060555).

CHAPTER 3

Investigation of Tumor-Stromal Communication Using a Screening Platform to Identify Short-Range Interactions

3.1 Abstract

Conventional methods for studying paracrine signaling may not be sensitive to short-range effects resulting from signal dilution or decay. Gap comb co-culture, however, maintains two cell populations in microscale proximity, while still allowing individual populations to be quickly retrieved for cell-specific readouts by standard high-throughput assays. We show that this method reveals gene expression changes, and thus paracrine interactions, in a tumor-stromal crosstalk model that are not detectable by conditioned media transfer or porous cell culture inserts. By co-culturing cells with each of the three methods and comparing the patterns of gene expression, this can serve as a screening technique to identify effects of short-range communication. Thus we demonstrate a tool for investigating an important class of intercellular communication that may be overlooked in conventional biological studies.

3.2 Introduction

Paracrine cell-cell signaling can be acutely range-dependent due to mechanisms such as ultrasensitivity in the response to a concentration gradient[48] or rapid signal decay, for example by reactive oxygen species.[49] *In vitro* studies of cell-cell signaling often employ compartmentalized culture models instead of mixed co-cultures in order to avoid confounding the readouts from two different cell populations. The most common approaches are conditioned media transfer between populations in separate wells, and the

use of porous cell culture inserts that separate two populations by a semi-porous membrane and a distance of about 1mm. However, these conventional approaches may not be sensitive to short-range paracrine effects.

Previous comb studies focused on the importance of contact-dependent signaling, however, the data also suggested that cells co-cultured in close proximity displayed enhanced viability compared to cells co-cultured at a greater distance from each other.[13,30] In addition, the previous chapter provided evidence that cellular state can be maintained by short-range communication, while it is lost with only longer-range signaling. It has also been reported that Hedgehog signaling between prostate tumor cells and myofibroblasts was observed only when the populations were cultured in close proximity at a separation of 500 μm by using a microfluidic culture platform.[25]

While these previous studies point to the importance of paracrine signaling range, there has not existed a high-throughput technique to screen for distance-dependent effects. In this chapter, we combine comb culture substrates with a quantitative reverse transcriptase polymerase chain reaction (qRT-PCR) array to identify gene expression changes resulting from tumor-stromal crosstalk. We compare gene induction on our platform with conventional conditioned media transfer and porous membrane inserts in an effort to discover distance-dependent gene expression patterns.

3.3 Materials and Methods

Cell Culture

HT1080 fibrosarcoma cells were obtained as a gift from Dr. Eric Stanbridge and were cultured in DMEM (Genesee, San Diego, CA) supplemented with 10% fetal bovine serum (FBS) (Fisher, Pittsburg, PA) and 1% Penicillin-Streptomycin (Genesee) and used

between passages 80 and 90. Normal human lung fibroblasts (Lonza, Basel, Switzerland) were cultured in M199 (Genesee) with the same supplements and used between passages 13 and 14.

Comb Co-culture

Comb substrates were coated with 1% gelatin (Sigma Aldrich, St. Luis, MO) for 30 minutes. Tumor cells (4×10^5 in 1 mL culture media) and fibroblasts (1×10^5 in 1 mL culture media) were seeded separately onto comb pairs locked together in contact in 12-well plates. After 6 h, the combs were moved to a new well with fresh culture media and separated to the gap configuration. After an additional 6hr, the cells from the back portion of the comb were removed by a cell scraper (Fisher) to leave only the cells adhered to the comb teeth. The comb pairs were gently dipped twice in PBS, incubated in a new well with fresh media for 3hr, and dipped twice in fresh PBS to eliminate detached cells. Combs were then paired and interlocked with either a comb plated with the same cell type (comb monoculture) or a comb with the opposing cell type (comb co-culture) in 2 mL of EGM-2 (Lonza), with a separation of 80 μm between the combs. After 48hr, comb pairs were decoupled, quickly washed in PBS, and grouped with other combs from the same experimental condition. Cells were then lysed off the combs and collected. Material from 18 combs (for fibroblasts) or 12 combs (for tumor cells) was used for each condition of each replicate experiment.

Cross-Contamination Tests

Combs were prepared as described for comb co-culture. After the cell-scraping step, half of the combs were incubated in DiI (LifeTechnologies) for 3hr for cell labeling. Labeled combs were paired with unlabeled combs containing the opposing cell type for 48hr.

Fluorescence and brightfield reflective light imaging was performed every 24hr using an upright Olympus U-TVO.63XC microscope to measure cross-contamination of the stained cells. Stained cells appearing on the unstained comb were counted, and this number was divided by the total number of cells on the unstained comb to calculate percent cross-contamination.

Conventional qRT-PCR Assays

RNA was isolated using a Qiagen RNeasy kit (Valencia, CA) and cDNA was generated using the Biorad Iscript cDNA Synthesis system (Hercules, CA). Primers were synthesized by IDT (San Diego, CA). Primer sequences are reported in Table S2. Gene expression levels were normalized to hypoxanthine-guanine phosphoribosyltransferase (HPRT).

qRT-PCR Array

RNA was isolated and cDNA was prepared as described above. Samples were added to the Human Angiogenesis RT^2 Profiler PCR array (Qiagen) and qRT-PCR was performed. Gene expression levels were normalized to the geometric mean of the 6 housekeeper genes on the array.

Conditioned Medium Co-culture

For experiments on comb substrates, conditioned medium was collected from fibroblasts (1.5×10^5 cells per comb pair) or tumor cells (8×10^5 cells per comb pair) plated onto paired combs. For experiments performed under standard conditions, conditioned medium was collected from fibroblasts (1.5×10^5 cells per well) or tumor cells (3×10^5 cells per well) cultured for 48hr directly in a well of a 12-well plate in 2 mL of EGM-2. The target cells to be cultured in this conditioned media were plated on comb substrates as described above for comb co-cultures, or directly in 12-well plates with 7.5×10^4 cells per well for

fibroblasts and 1 x 10^5 cells per well for tumor cells. After 48hr of culture in conditioned medium (2 mL of per well), the cells were washed and cell lysate was collected. Monoculture controls were set up identically but received fresh medium in place of conditioned medium. Cell material from 18 combs (for fibroblasts) or 12 combs (for tumor cells) was used for each condition of each replicate experiment. For conventional cultures without combs, cell material was pooled from 2 fibroblast wells or 1 tumor well for each condition of each replicate experiment.

Transwell Co-culture

5 x 10^4 fibroblasts or 5 x 10^4 tumor cells were seeded in each 8 μm Transwell insert (Millipore, Billerica, MA) in 12-well plates with 2 mL of medium per well. Target cells were plated on comb substrates as described above, or directly in 12-well plates at 7.5 x 10^4 cells per well for fibroblasts and 1 x 10^5 cells per well for tumor cells. The Transwell inserts were transferred to wells containing appropriate target cells and fresh EGM-2 medium (2 mL). Monoculture controls were set up identically but did not receive Transwell inserts. After 48hr of culture, the Transwell inserts were removed, the target cells were washed, and cell lysate was collected. Cell material from 18 combs (for fibroblasts) or 12 combs (for tumor cells) was used for each condition of each replicate experiment. For conventional cultures without combs, cell material was pooled from 2 fibroblast wells or 1 tumor well for each condition of each replicate experiment.

3.4 Results and Discussion

We chose a model system consisting of HT1080 human fibrosarcoma cells co-cultivated with human lung fibroblasts. This particular pairing was selected because the lung is a common site for fibrosarcoma metastasis.[51] Combs were individually plated with

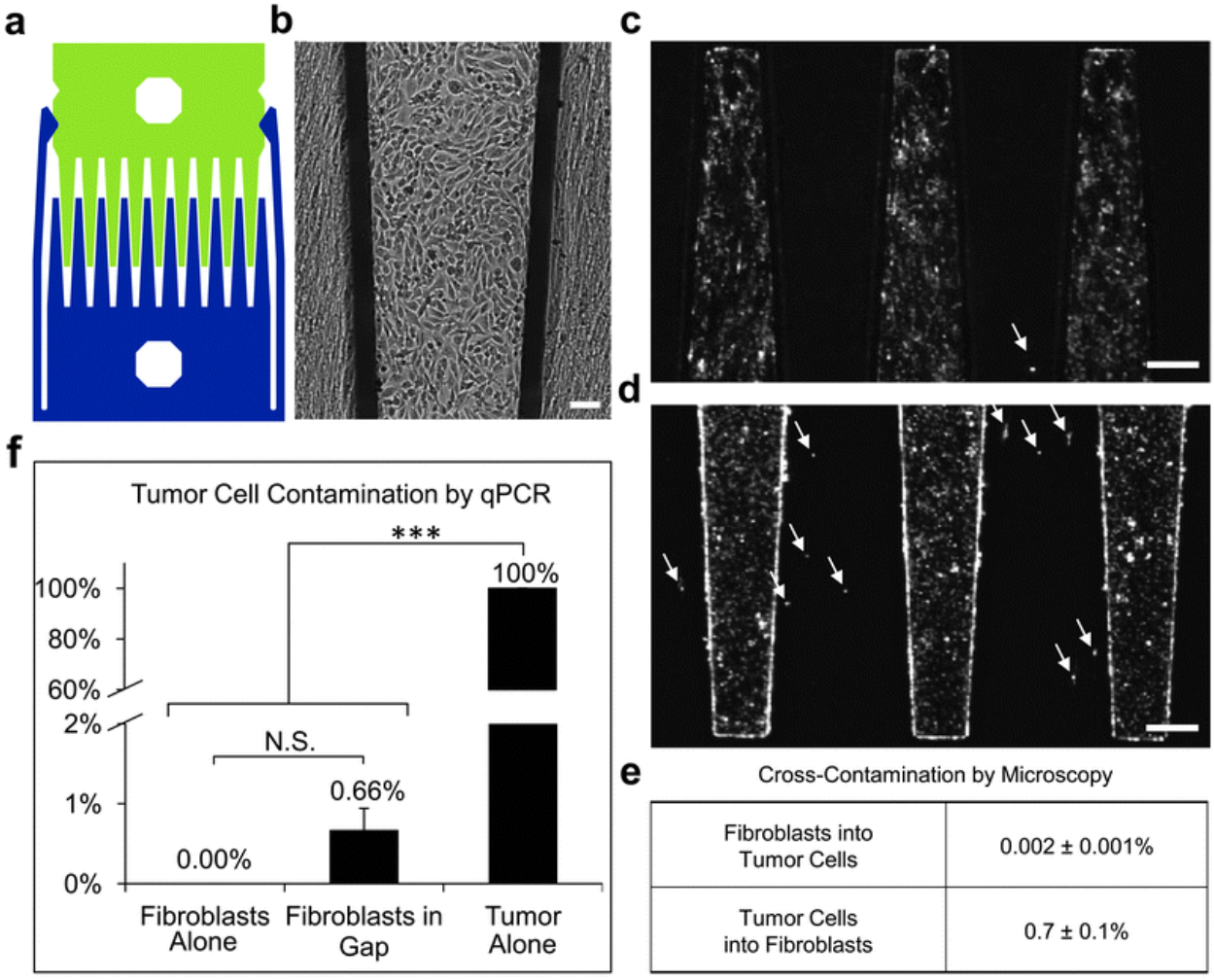

Figure 3.1. Comb substrates allow cells to be cultured in close proximity with minimal cross-contamination. (a) Diagram of device with paired combs locked into the gap configuration. (b) Brightfield reflected light image of HT1080 tumor cells (cobblestone cells) and human lung fibroblasts (elongated cells) in gap co-culture after 48hr, scale bar 100 mm. (c–d) Fluorescent images with arrows highlighting (c) a DiI-labeled fibroblast contaminating the tumor population, and (d) DiI-labeled tumor cells contaminating the fibroblast population in gap co-culture, scale bar 250 mm. (e) Quantification of fluorescent images shows minimal cross-contamination. (f) Minimal tumor contamination of the fibroblast population in gap co-culture, as determined by qRT-PCR for the tumor cell marker, TERT, relative to HPRT. Samples displaying statistically significant changes (Student's t-test) are indicated (*** = $p<0.005$) and relevant changes that are not significant are denoted (N.S.). Error bars are SEM.

pure populations, and then pairs were snapped together to form co-cultures with HT1080s and fibroblasts in close proximity but separated by a gap of 80μm (Fig. 3.1a). In order to verify that the tumor and fibroblast populations remained pure during this gap co-culture,

we used fluorescent labeling to track cross-contamination between the two populations (Fig. 3.1b,c). After 48hr, we measured 0.7% contamination of HT1080s in the fibroblast population, and 0.002% contamination of fibroblasts in the HT1080 population (Fig. 3.1d). Contamination of the fibroblast population by HT1080s was additionally verified by qRT-PCR quantification, using telomerase reverse transcriptase (TERT) as a tumor cell marker. TERT levels in lysate collected from the fibroblast combs after 48hr of gap co-culture corresponded to 0.66% contamination by HT1080 cells (Fig. 3.1e).

Given the ability to retrieve highly pure populations from gap co-cultures, we next assayed the gene expression changes induced in each population as a result of paracrine crosstalk during co-cultivation. Gap co-cultures were prepared alongside monoculture controls in an identical gap configuration but with a single cell type on both combs. After 48hr, the comb pairs were separated to retrieve pure tumor and fibroblast populations and the cells were immediately lysed off the combs. Following RNA isolation and cDNA generation, the samples were analyzed with a qRT-PCR array to measure the expression of 84 genes associated with tumor progression (Fig. 3.2a). Genes of interest were identified based on the magnitude and statistical significance of the differences in expression level in co-culture compared to monoculture. The expression of these genes was then quantified by conventional qRT-PCR in order to validate the results of the array. Specifically, we examined the expression of ANGPTL3, ANGPTL4, CXCL3, ID1, IL-1β, IL-6, IL-8, THBS1, and VEGFA in the tumor cells, and the expression of HPSE, ID1, and KDR in the fibroblasts. Although some of these genes of interest proved to be false positives, others were successfully validated by conventional qRT-PCR. In the HT1080s, the expression levels of CXCL3, ID1, IL-6, and IL-8 were significantly increased during gap co-culture relative to

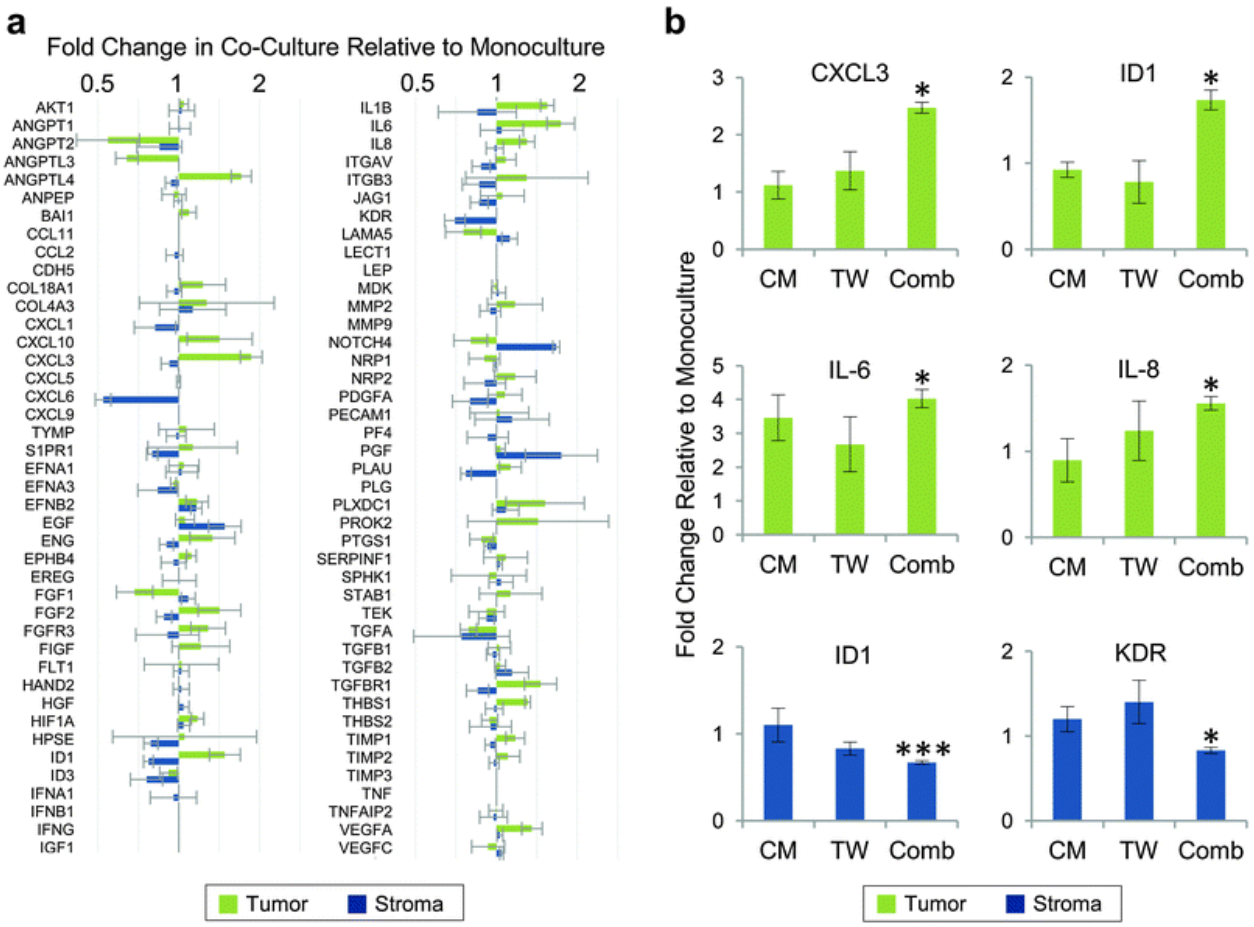

Figure 3.2. (a) Cell-specific gene expression changes on comb substrates, assayed by the qRT-PCR array. Fold change in co-culture relative to monoculture is displayed for both HT1080 tumor cells (green) and lung fibroblasts (blue). (b) Gene induction as a function of cell proximity. Quantification by conventional qRT-PCR of gene expression in conditioned medium (CM), Transwell (TW), and comb gap (Comb) co-cultures. In all conditions, all assayed cells were cultured on comb substrates. Samples displaying statistically significant changes (Student's t-test) versus monoculture controls are indicated (* = $p < 0.05$, *** = $p < 0.005$). Error bars are SEM, with n = 3 in all cases.

monoculture controls, by 2.54-fold, 1.72-fold, 4.38-fold, and 1.56-fold, respectively (Fig. 3.2b). In the fibroblasts, the expression levels of ID1 and KDR were significantly decreased during gap co-culture relative to monoculture controls, by 0.67-fold and 0.83-fold respectively (Fig. 3.2b).

In order to determine whether the close proximity of gap co-culture plays a role in driving the observed changes in gene expression, we repeated the experiment by using

conditioned media transfer (CM) and Transwell porous membrane inserts (TW) to achieve paracrine signaling. Here, we focused on the six validated genes from above and used conventional qRT-PCR for quantification. Gene expression in the presence of paracrine crosstalk was normalized to monoculture controls. In order to control for substrate effects, all cells that were assayed for gene expression were cultured on combs. In terms of proximity, cells were most distant in conditioned media transfer, at an intermediate separation in Transwell culture, and closest in gap culture on comb substrates.

A striking proximity effect was observed for CXCL3 and ID1 in HT1080s, with significant induction observed in gap co-culture with lung fibroblasts, but no change in conditioned media or Transwell cultures (Fig. 3.2b). Likewise, IL-8 expression in HT1080s exhibited greater induction in gap co-culture, but IL-6 expression appeared to be less sensitive to proximity. In the fibroblasts, a weaker proximity effect was observed, with ID1 and KDR moderately inhibited relative to monoculture only in gap co-culture. The conditioned media and Transwell experiments were also repeated on conventional substrates, with similar trends generally observed (Fig. 3.S1).

In our model system, we observed 5-fold greater baseline expression of CXCL3 in the stromal cells versus the tumor cells (Fig. 3.3a). In short-range co-culture, tumor expression of CXCL3 increased by 2.5-fold, but without a cell-specific assay, this strong change would be largely masked by the stromal signal (Fig. 3.3a,b). Thus, the ability to retrieve pure populations out of co-culture is critical for enabling certain crosstalk responses to be observed. CXCL3 has been associated with an aggressive metastatic phenotype[52,53] and also implicated as an autocrine growth factor.[54] Therefore, our observations are consistent with stromal induction of tumor progression through both

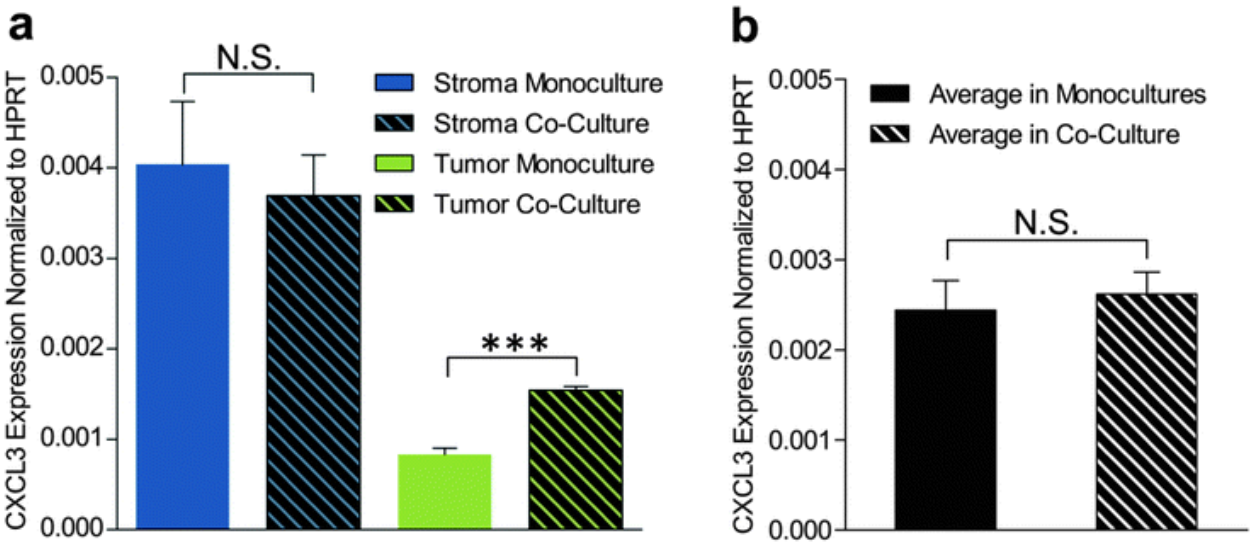

Figure 3.3. Masking of cell-specific gene expression changes in mixed co-culture. (a) Baseline CXCL3 expression in fibroblasts (blue) is almost 5 times higher than in HT1080 cells (green). Upon co-culture, the expression of CXCL3 in fibroblasts is unchanged (hatched blue), while HT1080 expression is significantly increased (hatched green). Here, upregulation of CXCL3 in HT1080s is clearly observed due to the cell-specific readout. (b) In a mixed co- culture without cell-specific readouts, the average CXCL3 expression (hatched) would not be significantly different from the average of CXCL3 expression in the two monoculture populations (black), and thus the upregulation in HT1080s would not be detected. Samples displaying statistically significant changes (Student's t-test) are indicated (*** = $p < 0.005$) and relevant changes that are not significant are denoted (N.S.). Error bars are SEM, with n = 3.

direct and indirect mechanisms: directly by paracrine secretion of CXCL3, and indirectly by stimulating tumor cells to secrete autocrine CXCL3.

The array data indicated strong induction of Notch4 in the fibroblasts, and this result was validated with conventional qRT-PCR (10.5-fold). However, Notch4 expression was 555-fold higher in the HT1080s than in the fibroblasts. Since we measured approximately 1% contamination of HT1080s into fibroblasts, it was possible that the observed increase in Notch4 mRNA in the fibroblast lysate was largely due to tumor contamination. Hence, Notch4 was discarded as a gene of interest. With any cell pairing, it will be important to quantify cross-contamination to guard against false positives.

Unfortunately, we were not able to explore all of the potential genes of interest (such as CXCL6 and PLAU in fibroblasts) due to the limited volume of RNA isolate that could be extracted. Due to the limited surface area of the comb device,[13] cells needed to be pooled from up to 18 combs per condition in order to obtain sufficient RNA quantity. Sample volume was a particular issue for the fibroblasts, which yielded less total RNA than the tumor cells. By employing new molecular analysis techniques such as barcoded hybridization (Nanostring nCounter) and RNA sequencing, it will be possible to profile larger numbers of genes from smaller sample volumes.

3.5 Conclusion

The comb device enables separation of co-cultures into pure populations, which can then be analyzed by a wide variety of standard approaches. Other methods for obtaining cell-specific readouts have included xenotypic co-cultures with species-specific primers,[55] mass spectrometry of proteins from cells labeled with heavy isotopes,[56,57] or genetic modification of cells to produce labeled mRNA,[58] but these approaches offer less flexibility in terms of cell types and assays. Fluorescence-activated cell sorting can also produce purified populations from a mixed culture, but dissociation into single-cell suspensions is not always possible and signals can degrade during the lengthy process. Due to these disadvantages, along with considerations of cost and difficulty, compartmentalized co-culture techniques such as conditioned media transfer and porous membrane inserts remain heavily utilized in the current literature. As we have demonstrated, however, significant interactions can go completely undetected by these conventional methods. It is possible that a substantial subset of cell-cell interactions have been previously overlooked due to the limitations of conventional tools in detecting short-range paracrine signaling.

Our method provides a useful technique for exploring this class of intercellular communication.

3.6 Supplementary Information

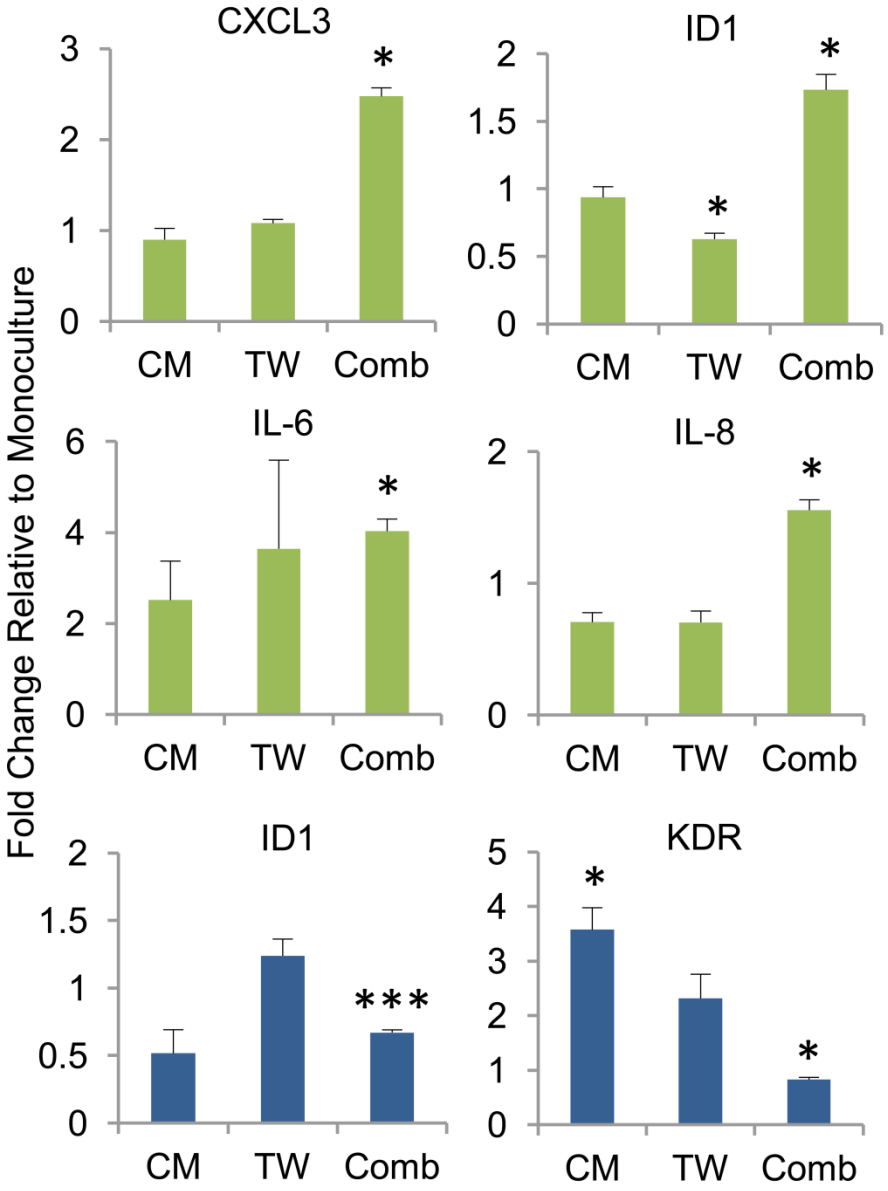

Figure S3.1. Gene induction as function of cell proximity. Quantification by conventional qRT-PCR of gene expression in conditioned media (CM), Transwell (TW), and comb gap (Comb) co-cultures. Here, CM and TW were performed conventionally, with cells in normal culture wells without comb substrates. In general, the trends are similar to Figure 2, in which all conditions were performed on comb substrates. Samples displaying statistically significant changes (Student's t-test) versus monoculture controls are indicated (* = $p < 0.05$, *** = $p < 0.005$). Bars are color-coded green for tumor-specific gene expression and blue for fibroblast-specific gene expression. Error bars are SEM.

Gene	Forward 5' to 3'	Reverse 5' to 3'
ANGPTL3	CCAAGCCAAGAGCACCAAGAACT	CTCCACACTCATCATGCCACCAC
ANGPTL4	GTCCTCCGCGTCTCCAGTCCT	CATCTCGGGCAGCCTCTTTCTT
CXCL3	TGCCCTTACCAGAGCTGAAAATGA	AAGAGAAACGCTGCAGAATGGACA
HPRT	GACCAGTCAACAGGGGACA	GTGTCAATTATATCCTTCCACAA
HPSE	CCCGCCTCAGCCTCTCAAAGT	GCCTCGGCCTCCCAAAGTG
ID1	CCTCAACGGCGAGATCAG	CGCTTCAGCGACACAAGAT
IL-1β	AGGCCGCGTCAGTTGTTGTG	TATATCCTGGCCGCCTTTGGTC
IL-6	CCCCAGTACCCCCAGGAGAAG	CTGCGCAGAATGAGATGAGTTGTC
IL-8	AGAAACCACCGGAAGGAACCATC	GCAACCCTACAACAGACCCACAC
KDR	GAGCCGGCCTGTGAGTGTAAAAA	AGGAGTTGGGGGTGTGGATGC
TERT	GGTCATCGCCAGCATCATCAAA	ACGGCTGGAGGTCTGTCAAGGTAG
THBS1	GCCACGGCCAACAAACAGGT	ACAGCGGTCTCCCACATCATCTC
VEGFA	AGATGTCCCGGCGAAGAGAAGA	GGGAGGGCAGAGCTGAGTGTTAG

Table S3.2. Primer sequences employed for qRT-PCR. These were employed for the validation experiments and may be different from the primers in the qRT-PCR arrays.

3.7 Acknowledgments

This work was originally published in Integrative Biology, 2014 and is reproduced by permission of The Royal Society of Chemistry. It was performed with the help of co-authors Monica Y. Kim, Christopher C. W. Hughes, and Elliot E. Hui. It was supported in part by the Chao Family Comprehensive Cancer Center (CFCCC) through an NCI Center Grant (P30A062203). E. E. H. was supported by the American Cancer Society (ACS/IRG 98-279-07). K. H. S. was supported by fellowships from the NSF (GRFP) and the NIH (T32-HD060555). C. C. W. H. is supported by NIH grant RO1HL60067.

CHAPTER 4

Deeper Investigation of Tumor-Stromal Interactions Using Comb Co-culture: Tumor Communication Triggers Fibroblast Migration and Proliferation Through WNT-dependent and WNT-independent Mechanisms

4.1 Abstract

Tumor-stromal communication strongly influences cancer progression and fibroblasts in particular are known to regulate tumor growth and metastasis. Tumor cells recruit fibroblasts to the tumor microenvironment to allow these interactions to occur, but little is known about the signaling factors and intracellular pathways that mediate recruitment. We employ comb co-culture, because of its sensitivity to short- and long-range communication and its ability to rapidly manipulate cells in co-culture, as well as other conventional culture assays to study how tumor cells stimulate fibroblast migration. We report for the first time that tumor-induced fibroblast migration is dependent on canonical WNT signaling. We also show evidence that urokinase plasminogen activator activity regulates this WNT-dependent effect.

4.2 Introduction

Interactions between tumors and the surrounding stroma are known to alter the course of tumor development and progression.[59] Many studies have investigated how stromal cells, especially fibroblasts, effect tumor cell behavior, but by comparison, fewer focus on how cancer cells modify their surroundings and affect nearby stroma. Fibroblasts are one of the most abundant populations in the microenvironment.[60] However, the

majority of the fibroblasts were not native to the region prior to the tumor, but rather appeared as the tumor developed.[61]

Studies suggest that some of the fibroblasts originate from bone marrow cells,[62] but other evidence indicates that some of the fibroblasts may be actively recruited to the tumor.[61] A few of the tumor-derived growth factors and cytokines involved in this recruitment have been identified,[59] but much more investigation into the underlying mechanisms needs to be performed.

Here, we take advantage of the unique capabilities of comb co-culture—sensitivity to both long and short-range communication and rapid manipulation of cells in co-culture—to study the effect of tumor-stromal interactions on fibroblast migration. We show for the first time that tumor cells trigger fibroblast migration via canonical WNT signaling and reveal that this effect is mediated through urokinase plasminogen activator (uPA) activity. We also found that tumor cells increase fibroblast proliferation through WNT-independent pathways. With better understanding of the inter- and intracellular signaling that causes this behavior, the collection of possible cancer drug targets can be expanded to include more stromal components and thus improve the chance of finding a successful therapy.

4.3 Material and Methods

Cell Culture

HT29 colon cancer cells and CCD-18CO colon fibroblasts were obtained from ATCC and cultured in Gibco RPMI (LifeTechnologies) supplemented with 10% Gibco FBS (LifeTechnologies) and 1% Penicillin-Streptomycin (Genesee) between passages 8-37 and passages 12–30, respectively. Fibroblasts were activated to mimic myofibroblasts by

treating flasks of them with TGFβ (10ng/mL, Peprotech, Rocky Hill, NJ) for 4 days, changing media and TGFβ after the first 48hr. TGFβ was also present in the media during seeding and during the 24hr exposure to serum free media before experimental culture described below.

Comb Co-culture

Fibroblasts (2 $x10^5$) or HT29 tumor cells (1 $x10^6$) were seeded overnight in culture media into wells of 12-well plates containing combs. For combs that would be used in Nanostring gene expression assays, cells were removed from the back portion of combs using a cell scraper so that only cells on the comb fingers remained. This was done because we wanted to mainly measure gene expression changes due to tumor-fibroblast communication. Unattached cells were removed by gently dipping combs into HBSS twice and combs were placed in new wells containing serum free (SF) media (RPMI with 0.1% BSA (SeraCare, Milford, MA) freshly prepared for each experiment). For the cell invasion comb experiments, Dio or DiI (LifeTechnologies) was added to the SF media so that the cells could be fluorescently labeled and their invasion into the adjacent population could be easily observed. After 24hr of exposure to SF media, combs were washed again as before and were combined in new wells containing new SF media to start contact-mode co-culture for invasion experiments or gap-mode co-culture for gene expression experiments. For invasion experiments, fluorescent images of the combs were taken at 0hr and then at 48hr using an upright Olympus U-TVO.63XC microscope. For gene expression experiments, combs were co-cultured for 3, 6, 12, 24, 36, or 48hr and then separated, washed, and lysed with RLT lysis buffer (Qiagen) in different wells so that gene expression could be assayed

for each cell population individually. Material from four combs per cell type and condition was pooled for Nanostring analysis.

Conditioned Media Generation

Fibroblasts or tumor cells were seeded in culture media into wells of 12-well plates overnight. Unattached cells were removed by washing with HBSS twice and SF media was added the wells. After 24hr of exposure to SF media, monolayers were washed again, and new SF media was added with or without LGK974 (100nM, XcessBio, San Diego, CA) to start generating conditioned media. The conditioned media was collected after 48hr, sterile filtered, diluted 1:1 in SF media, and used immediately in experiments.

Conditioned Media Culture

Monolayers of fibroblasts were prepared as described above for the generation of conditioned media. Instead of conditioning media for 48hr for collection, monolayers were cultured in SF media or conditioned media in the presence or absence of LGK974 (100nM, XcessBio, San Diego, CA), CHIR99021 (3μM, Abcam, Cambridge, MA), XAV939 (10μM, Sigma Aldrich, St. Louis, MO), or UK122 (200nM, VWR, Radnor, PA) for 48hr. For gene expression analysis, cells were lysed. For scratch wound healing experiments, a scratch was made across each monolayer with a p1000 pipette tip and the cells were washed twice with HBSS prior to culture in the appropriate media. Brightfield images of each monolayer were taken at 6 different locations along the scratch at the start of culture and the same locations were imaged again after 48hr using a Nikon Eclipse TE200 microscope. The surface area of the open region of the scratch in each location at 0hr and 48hr was compared using ImageJ to determine the amount of scratch closure. For mitomycin C experiments, monolayers were

treated for 4 mins with mitomycin C (0.01 mg/ml, Sigma Aldrich) prior to being scratched and washed.

Gene Expression Assays

RNA from each population from co-culture and control culture (same cell type cultured on adjacent combs) for each time point was isolated from lysate using the RNeasy Micro Kit (Qiagen) and subjected to the Nanostring assay using the Stem Cell code set (Seattle, WA). Raw data was normalized to the geometric mean of the 6 housekeeper genes on the panel using the nSolver Nanostring software. In Excel, the average of the read counts for the negative control probes was subtracted as background from the normalized data and genes that did not have read counts above the threshold (2 standard deviations of the negative control probes) for at least half of the time points were not included in further analysis. Read counts in co-culture were normalized to those in control culture and read counts of TGFβ-treated fibroblasts were normalized to those from untreated fibroblasts. Gene Set Enrichment Analysis[63] was performed using settings for continuous phenotype to identify genes that were generally upregulated (Score ≥ 2), generally downregulated (Score ≤ -2), increased over the time course (Score ≥ 0.6), or decreased over the time course (Score ≥ 0.6). GSEA was also performed to find gene sets from the C2 collection of the Molecular Signatures Database that were enriched (FDR < 0.25) in the Nanostring data.

For qRT-PCR assays, cDNA was generated using the Biorad Iscript cDNA Synthesis system (Hercules, CA) and primers were made by IDT (San Diego, CA) (Table S4.1). Gene expression was normalized to the housekeeper gene hypoxanthine-guanine phosphoribosyltransferase (HPRT).

BrdU ELISA

Fibroblasts (1 x 10^4) were seeded into wells of a 96-well plate in culture media overnight and washed and exposed to SF media for 24hr as described above. They were then cultured in 200μL of SF or conditioned media with or without LGK974, CHIR99021, or XAV939 for 48hr. Using the reagents and following the protocol provided in the BrdU Cell Proliferation ELISA kit (Abcam), Brdu was added 24hr before fixing the cells and then the cells were labeled with anti-BrdU primary antibody and horseradish peroxidase secondary antibody. Following the addition of tetra-methylbenzidine (TMB), absorbance was measured at 450nm using a Tecan microplate reader.

4.4 Results

Colon fibroblasts were co-cultured with colon tumor cells on combs in the contact configuration to study the effect of tumor cells on fibroblast invasion into the tumor microenvironment. After 48hr, fibroblast invasion into tumor cells was much higher than fibroblast migration into fibroblasts (Fig. 4.1). To better understand the invasive behavior of these cells, we assayed population-specific gene expression in gap control culture (same cell type on both combs) and in gap co-culture at 3, 6, 12, 24, 36, and 48hr using the Nanostring system. Gene Set Enrichment Analysis was performed to assess how fibroblasts respond to communication with tumor cells. According to the analysis, genes that seemed to be generally over- or underexpressed throughout the time course (*differentially expressed*) in co-culture compared to control culture belonged to pathways including the AP1, cell cycle, FOXM1, ATF2, FRA, E2F, and FGF pathways (Fig. 4.2). Genes whose expression appeared to increase over time in co-cultured fibroblasts compared to control

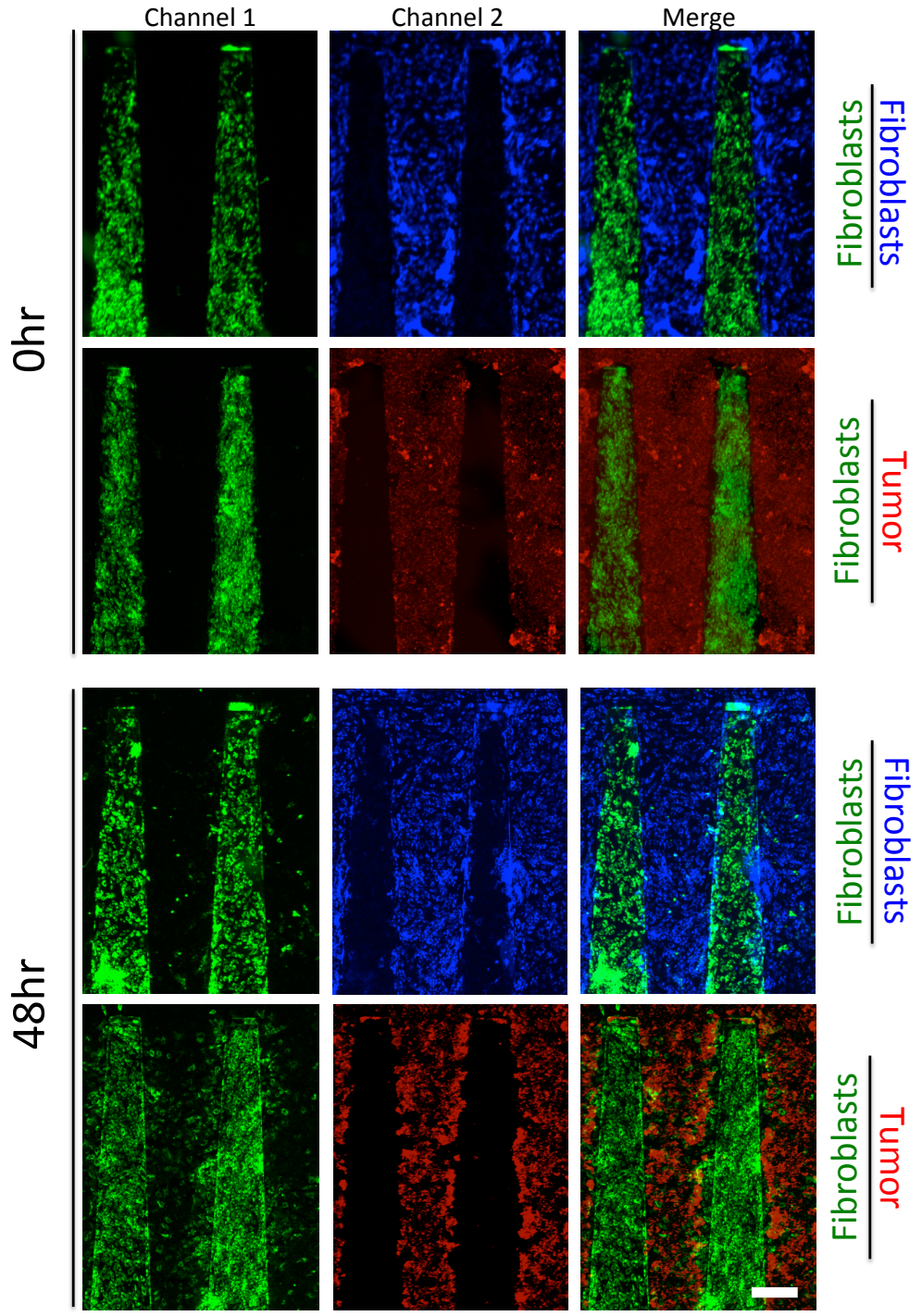

Fig. 4.1. Fibroblast invasion into tumor cells is greater than invasion into other fibroblasts. Fibroblasts (green) were co-cultured with other fibroblasts (blue) or with tumor cells (red) for 48hr on combs in the contact mode. More fibroblasts migrated onto the comb containing tumor cells as indicated by a higher number of green cells among red cells compared to green cells among blue cells.

fibroblasts belonged to the insulin receptor, cell cycle, FRA, WNT, FGF, AP1, and cell death pathways. Similarly, components of the hedgehog and WNT pathways appeared to decrease in fibroblasts co-cultured with tumor cells over time. Because the WNT pathway appeared to be modulated in fibroblasts co-cultured with tumor cells, and because WNT

Gene Set	False Discovery Rate
Differentially Expressed	
AP1 Pathway	0.015
Cell Cycle Transition	0.034
FOXM1 Pathway	0.037
ATF2 Pathway	0.100
FRA Pathway	0.146
E2F Pathway	0.165
FGF Pathway	0.230
Increasing Over Time	
Insulin Receptor Pathway	0.071
Cell Cycle Transition	0.111
FRA Pathway	0.139
WNT Pathway	0.162
FGF Pathway	0.200
AP1 Pathway	0.200
Cell Death Pathway	0.221
Decreasing Over Time	
Hedgehog Pathway	0.163
WNT Pathway	0.183

Table 5.2. Results of gene set enrichment analysis. The Nanostring data for the fibroblast populations was subjected to gene set enrichment analysis (GSEA) to identify signaling pathways whose components are affected by co-culture with tumor cells. Components of pathways that were generally overexpressed or underexpressed throughout the time course, were considered differentially expressed. Pathways containing genes whose expression increased or decreased over the length of the time course were designated as increasing over time or decreasing over time, respectively. Only gene sets with false discovery rates (FDR) smaller than 0.25 were recorded.

signaling has been shown to affect migration and cancer progression,[64] we next investigated whether tumor cells increase fibroblast migration via the WNT pathway.

The Nanostring results indicated that the tumor cells express abundant amounts of WNT10A and WNT11, so we first determined whether tumor cell conditioned media alone, or uni-directional paracrine communication, would be sufficient to increase fibroblast migration. Fibroblasts were seeded into a tissue culture plate instead of a comb and a scratch wound healing assay was performed to measure the amount of fibroblast migration in response to different treatments. Closure of the scratch was significantly higher in

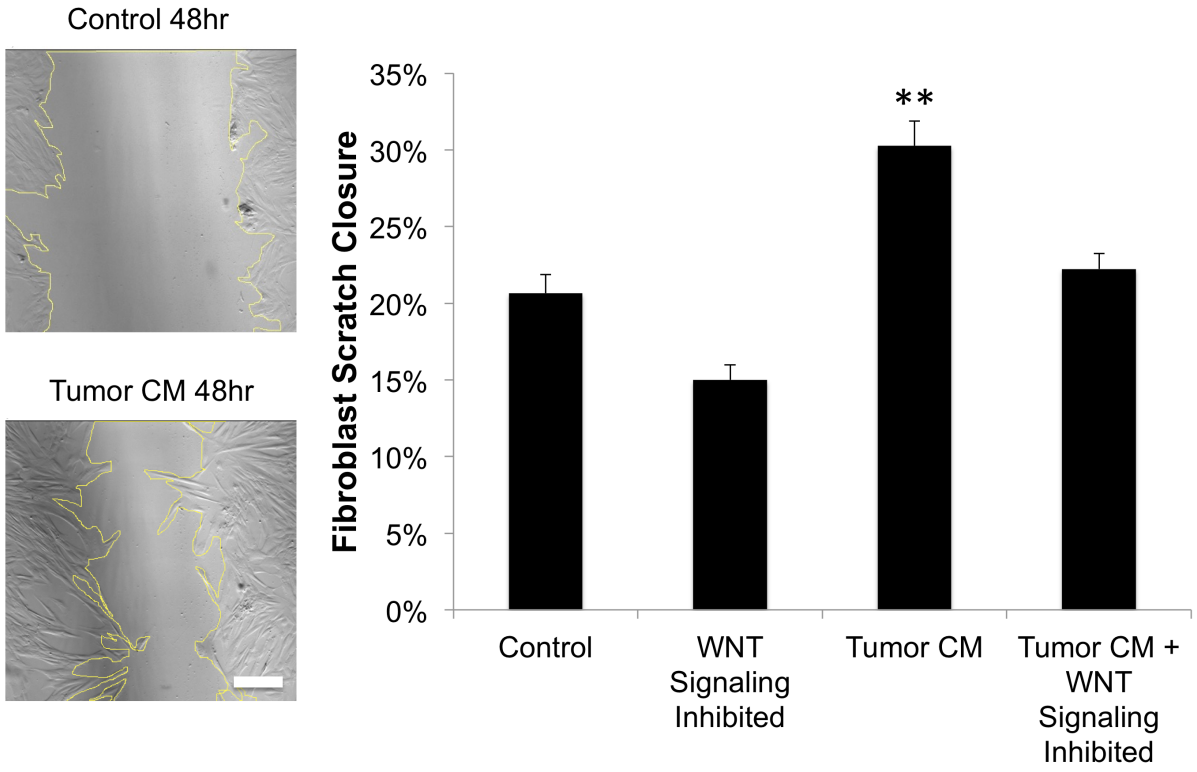

Figure 4.3. WNT signaling is required for enhancement of fibroblast migration by tumor factors. Fibroblast migration in response to serum-free media versus tumor conditioned media was assessed by scratch wound healing assay. Brightfield images of scratch closure after 48hr showed that tumor conditioned media resulted in greater migration, or closure of the scratch, and by quantifying percent scratch closure in tumor conditioned media in the presence of WNT signaling inhibitor XAV939 it was found that migration was reduced back to the level of the control, Scale bar is 250μm ** = $p < 0.01$.

tumor cell conditioned media compared to plain media (Control) (Fig. 4.3). Interestingly, when tumor conditioned media was present, but WNT signaling was inhibited in the fibroblasts by the addition of XAV939, scratch closure was reduced to back to the level of the control. Scratch closure was slightly lower after inhibiting WNT signaling in fibroblasts in the absence of tumor conditioned media, but the decrease was not significant. These

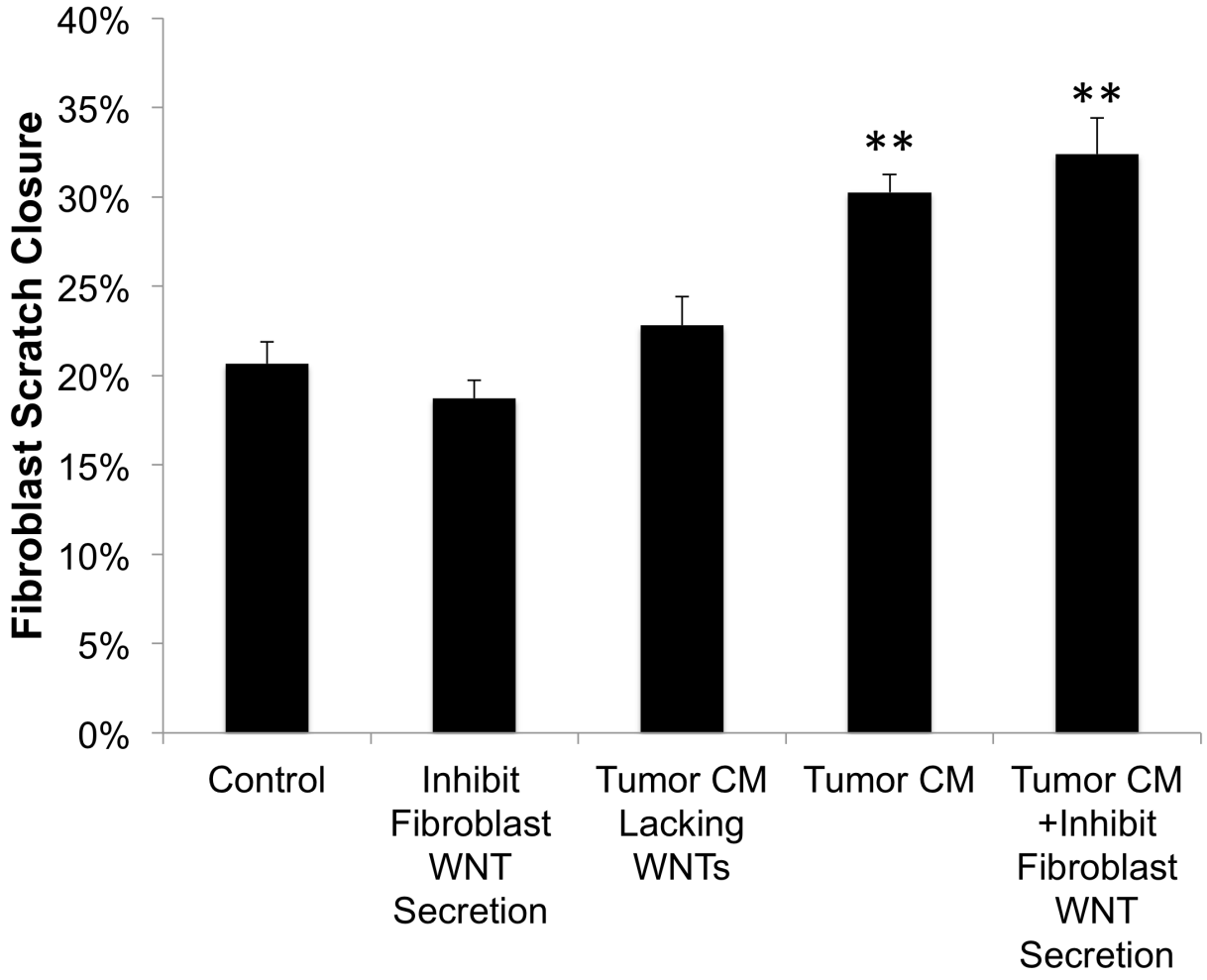

Figure 4.4. Tumor-derived WNTs stimulate fibroblast migration. WNT secretion inhibitor LGK974 was added during tumor conditioned media generation to produce conditioned media lacking WNTS or during the scratch assay to inhibit WNT secretion by fibroblasts in the presence or absence of tumor conditioned media. Only the absence of tumor-derived WNTs reduces fibroblast migration to the level of the control condition. ** = $p < 0.01$.

results suggest that tumor-derived factors increase fibroblast migration and that this effect requires WNT signaling in the fibroblasts.

In order to determine if the tumor-derived factors that are responsible for increasing fibroblast migration are actually WNT ligands or simply enhance an autocrine WNT feedback loop, LGK974 was used to block WNT ligand secretion. When WNT ligand secretion is blocked while the tumor conditioned media is being generated (Tumor CM Lacking WNTs) the fibroblasts no longer migrate more than the control (Fig. 4.4). However, inhibiting fibroblast WNT secretion does not affect migration in conditioned media. This indicates that tumor-derived WNT ligands are responsible for increasing fibroblast migration.

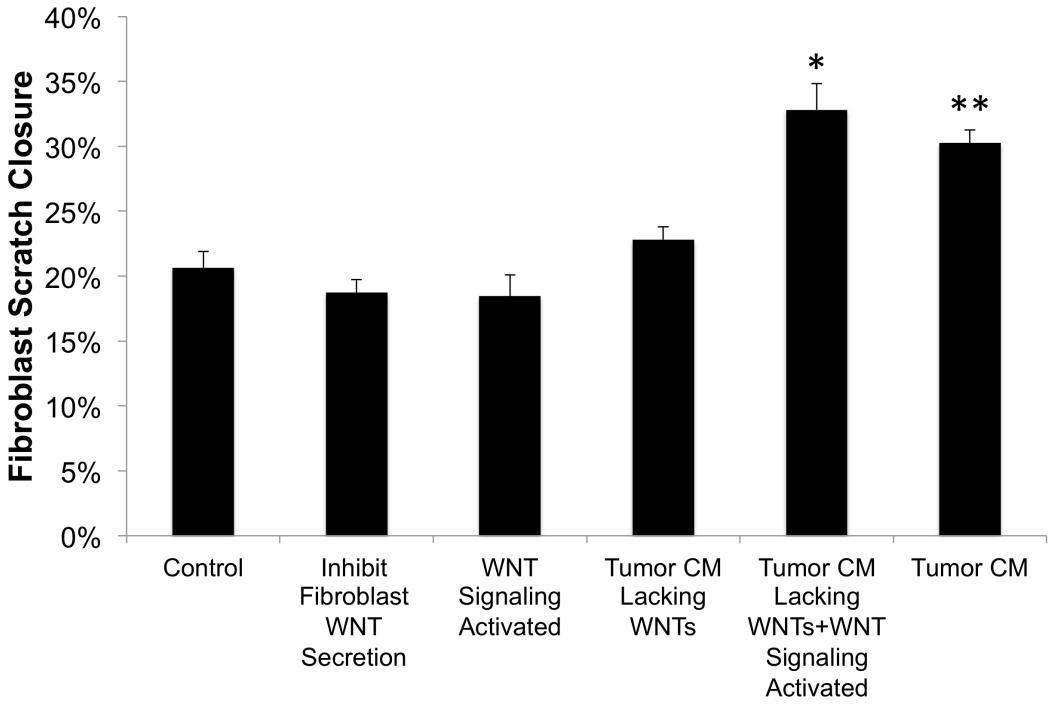

Figure 4.5. Tumor-stimulated fibroblast migration also requires mechanisms independent of canonical WNT signaling. Adding CHIR9902, a WNT signaling activator, to fibroblasts in serum-free media (WNT signaling activated) did not enhance migration, however, adding it to tumor conditioned media lacking WNTs rescued the higher migration phenotype, indicating that tumor factors besides WNTs are required. * = $p < 0.05$, ** = $p < 0.01$.

Next, an activator of WNT signaling, CHIR99021, was used to determine if WNT pathway activation alone in fibroblasts is sufficient to increase migration or if other signaling is required. When WNT signaling was activated in fibroblasts, scratch closure was not increased compared to the control (Fig. 4.5). Activating WNT signaling in fibroblasts cultured in tumor conditioned media lacking WNT ligands, however, rescued migration back to that of fibroblasts in tumor conditioned media. These results suggest that WNT pathway activation is necessary, but not sufficient, to increase fibroblast migration. Tumor-derived WNT ligands in addition to other tumor-derived factors act synergistically to enhance migration.

Since the data shows that tumor-derived WNT ligands in combination with other tumor factors enhance fibroblast migration by activating the WNT pathway, it would be expected that WNT target genes in fibroblasts are upregulated by conditioned media and that these genes regulate migration. Based on the Nanostring gene expression assay of fibroblasts in gap comb co-culture with tumor cells, several known WNT target genes were upregulated including urokinase-type plasminogen activator (uPA), CD44, FOSL, and cyclin D1. Standard RT^2 PCR on fibroblasts cultured in tumor conditioned media verified that the expression of these target genes was upregulated following exposure to tumor factors (Fig. 4.6,4.7). Furthermore, the upregulated expression of uPA, CD44, and FOSL was suppressed in conditioned media lacking WNT ligands, but was not suppressed in fibroblasts with inhibited WNT secretion cultured in tumor conditioned media (Fig. 4.6). This supports the claim that tumor-derived factors activate the WNT pathway in fibroblasts. In contrast, even though cyclin D1 expression was upregulated in conditioned media but not in conditioned media lacking WNT ligands, it was not upregulated in conditioned media when

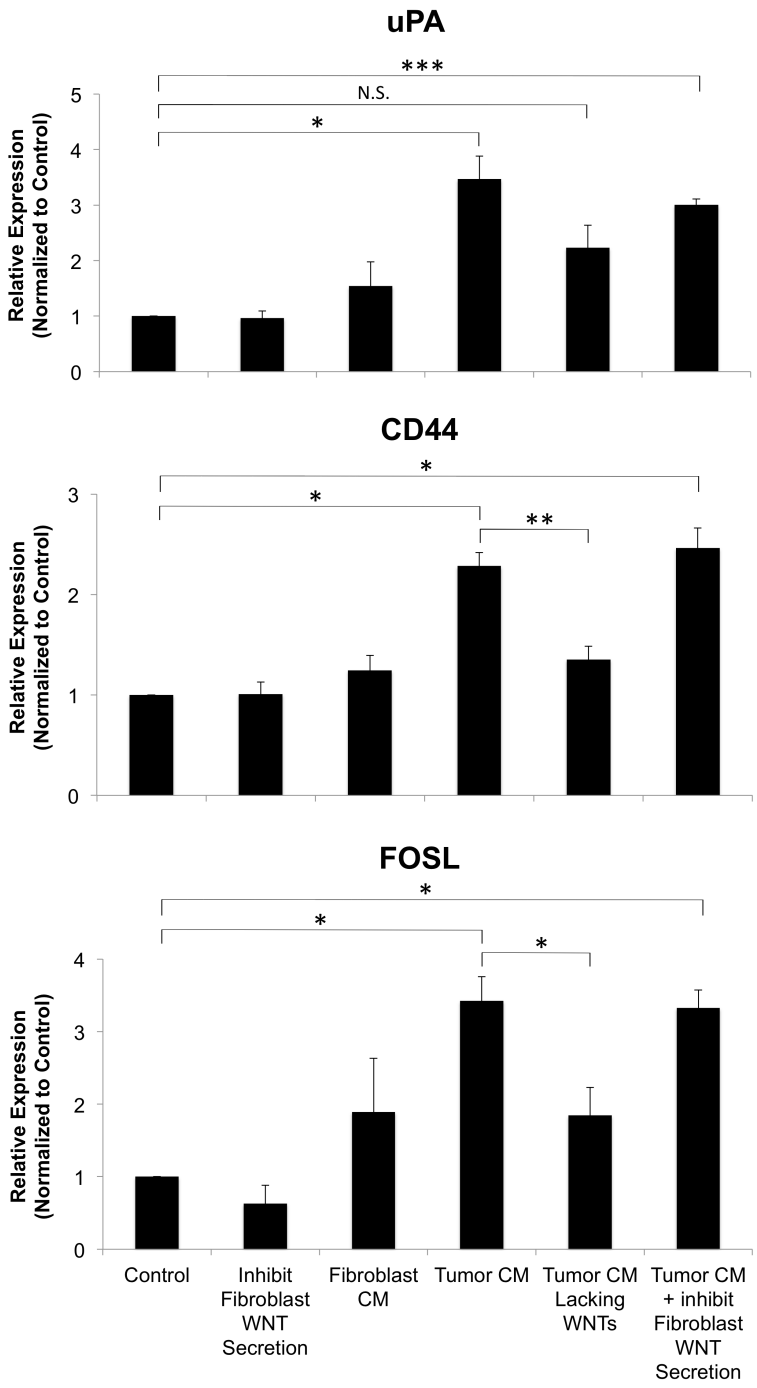

Figure 4.6. WNT target gene expression in fibroblasts depends on tumor-derived WNTs. Fibroblast monolayers were cultured in serum-free media (Control), fibroblast conditioned media (CM), tumor CM, tumor CM that was generated in the presence of WNT secretion inhibitor LGK974, or serum-free or conditioned media with LGK974. mRNA expression of uPA, CD44, and FOSL was quantified using qRT-PCR and normalized to HPRT expression and then to expression in the control condition. * = $p < 0.05$.

WNT secretion was inhibited in the fibroblasts (Fig. 4.7). It is possible that cyclin D1 expression requires tumor factors as well as fibroblast-derived WNT ligands.

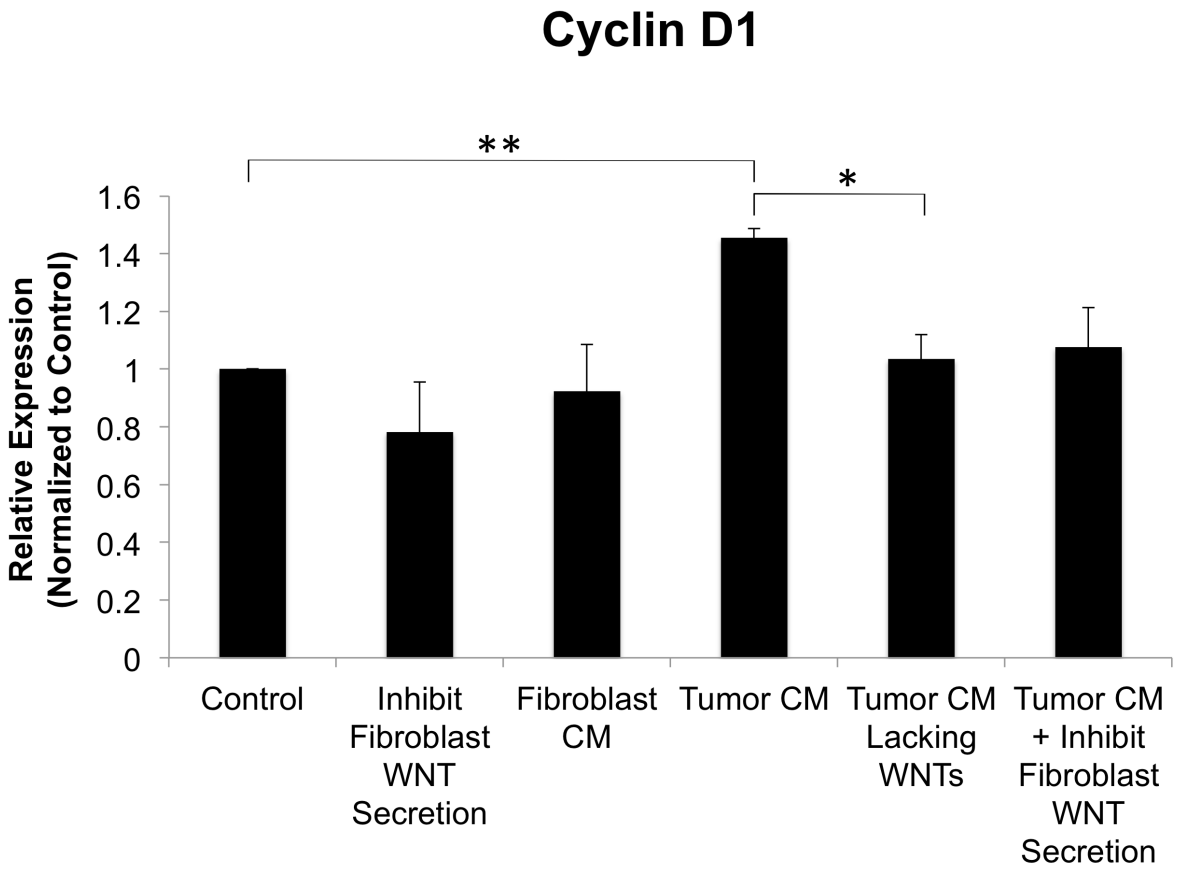

Figure 4.7. Cyclin D1 expressions is induced by tumor factors that are not WNT ligands. Fibroblast monolayers were cultured in serum-free media (Control), fibroblast conditioned media (CM), tumor CM, tumor CM that was generated in the presence of WNT secretion inhibitor LGK974, or serum-free or conditioned media with LGK974. mRNA expression of cyclin D1 was quantified using qRT-PCR and normalized to HPRT expression and then to expression in the control condition. * = $p < 0.05$, ** = $p < 0.01$.

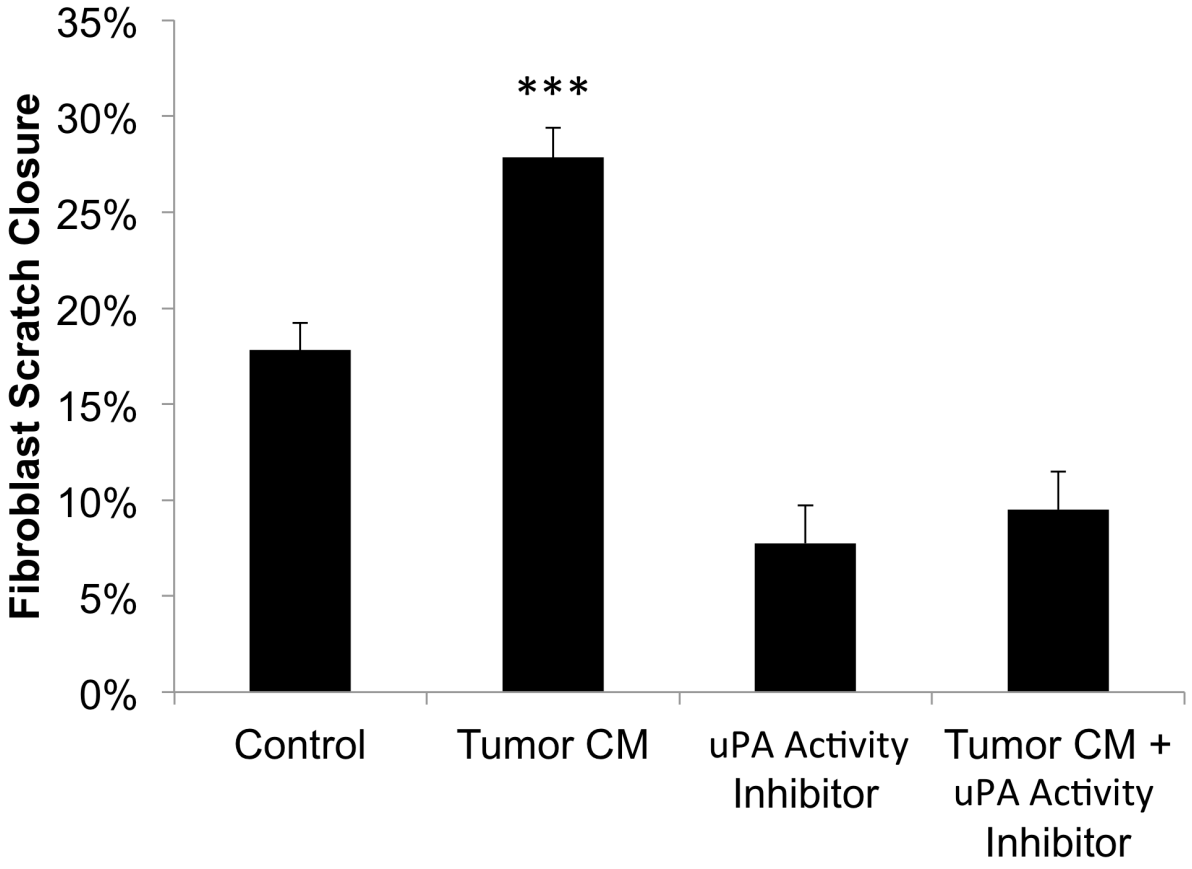

Figure 4.8. Tumor-stimulated fibroblast migration depends on uPA activity. Scratch assays were performed with fibroblasts cultured in serum-free media or tumor conditioned media in the presence or absence of uPA activity inhibitor, UK122. *** = $p < 0.005$.

Urokinase-type plasminogen activator (uPA), one of the WNT target genes that are overexpressed in co-cultured fibroblasts and in conditioned media, has been previously shown to affect migration.[65] Thus, uPA activity was blocked using UK122 to determine if uPA mediates the tumor-induced fibroblast migration effect. When uPA activity was inhibited in fibroblasts, tumor conditioned media no longer increased migration (Fig. 4.8) suggesting that tumor-derived WNT ligands upregulate fibroblast uPA which then mediates migration. Migration seems to be slightly reduced even when inhibiting uPA activity in fibroblasts cultured in control media, however it is not significantly different from the

control. This is not surprising because there is evidence that uPA is involved fibroblast migration in general.[66] uPA mediates migration through multiple mechanisms. It is secreted, but can be tethered to the cell surface by binding to its receptor uPAR, to either cleave plasminogen into plasmin to activate matrix remodeling proteins and growth factors[65] or induce intracellular signaling cascades by complexing with integrins[67] to coordinate cycles of cellular detachment and adhesion at the leading edge. Unless the fibroblasts or the tumor cells express plasminogen, it is not otherwise present in comb co-culture nor conditioned media culture. Therefore it would seem that uPA-dependent migration involves integrin binding and that UK122 not only inhibits uPA proteolytic activity, but may also interfere with uPA-uPAR-integrin interactions.

As earlier results indicate, tumor-derived WNT ligands act in conjunction with other tumor factors to induce migration. With this last data, uPA is also seems to be required. Thus, maybe the non-WNT tumor factor affects uPA activity, while the tumor-derived WNTs affect uPA expression. Soluble uPAR secreted from glioma cells has been shown to regulate stromal cell migration[68] by interacting with uPA and since the tumor cells used in this study, HT29, express soluble uPAR under various conditions[69,70] further investigation is needed to determine if this is the identity of the non-WNT factor.

Another WNT target gene that was overexpressed in co-culture and in conditioned media, CD44, mediates migration through the binding of extracellular matrix protein hyaluronin, interaction with integrins to achieve adhesion, and remodeling of the actin cytoskeleton. CD44 is known to have several transcript variants and the expression of transcripts with certain variant exons has been shown to enhance migration.[71] Thus, standard RT^2 PCR was performed to measure the expression of transcripts containing

variant exon v4, v6, v8, or v10. CD44v10 expression was significantly upregulated in fibroblasts cultured in conditioned media, however, the other variants were not significantly different from control levels. (Fig. 4.9) Interestingly, overexpression of CD44 transcripts containing exon v10 results in enhanced migration, invasion, or metastasis of colon, breast, head and neck, and melanoma cancer cells,[71-74] so it is possible that tumor-induced fibroblast migration may depend on CD44v10 overexpression as well. Transcripts containing v10 exon have been shown to induce migration by binding to β1 integrins and osteopontin,[75] so it could be possible that uPA and CD44 both associate with integrins to mediate tumor-induced fibroblast migration.

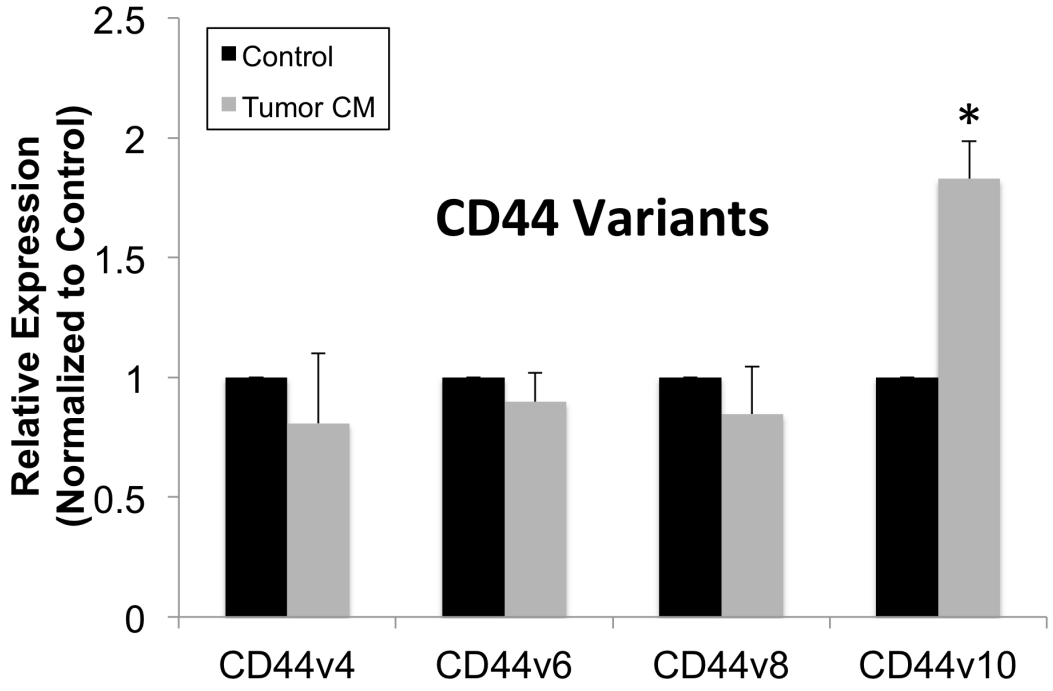

Figure 4.7. Transcripts containing variant exon CD44v10 are upregulated in fibroblasts by tumor factors. Fibroblast monolayers were cultured in serum-free media (Control) or tumor conditioned media (CM) and mRNA expression of variant exons 4, 6, 8, and 10 was quantified using qRT-PCR and normalized to HPRT expression and then to expression in the control condition. * = $p < 0.05$

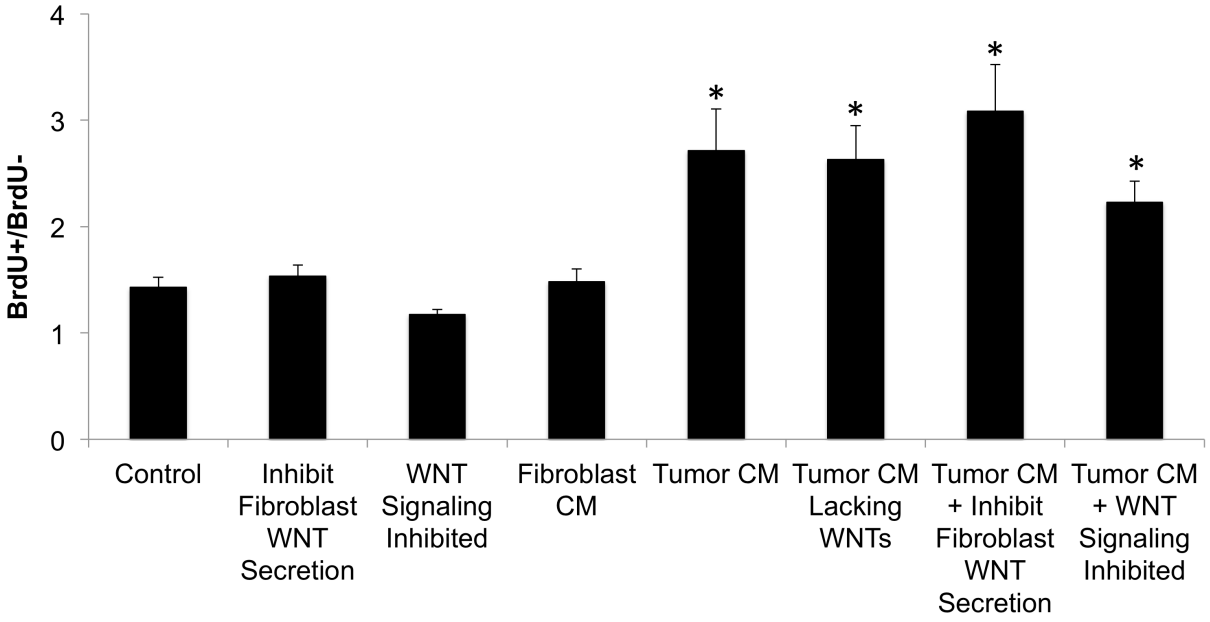

Figure 4.10. Tumor factors induce fibroblast proliferation through canonical WNT-independent methods. Fibroblast monolayers were cultured in 96-well plates in serum-free media, fibroblast conditioned media (CM), tumor CM, or tumor CM generated in the presence of LGK974 (tumor CM lacking WNTs) in the presence or absence of LGK974 or XAV939. After 24hr BrdU was added to the cultures and after an additional 24hr, the cultures were fixed and subjected to an ELISA for BrdU. Absorbance at 450nm was recorded and normalized to cultures not receiving BrdU. * = $p < 0.05$.

Because the GSEA analysis suggested that the cell cycle transition pathway was affected by co-culture with tumor cells and because cyclin D1 expression was among the genes upregulated by co-culture and tumor conditioned media, a BrdU incorporation assay was used to see if tumor-derived factors also promoted fibroblast cell division. Not only did conditioned media significantly increase cell division, but conditioned media lacking WNT ligands increased cell division as well (Fig. 4.10). In addition, cell division was higher in conditioned media when WNT secretion or WNT signaling was inhibited in fibroblasts (Fig. 4.10). Therefore, a tumor-derived factor increases fibroblast cell division, but not through a WNT-dependent mechanism.

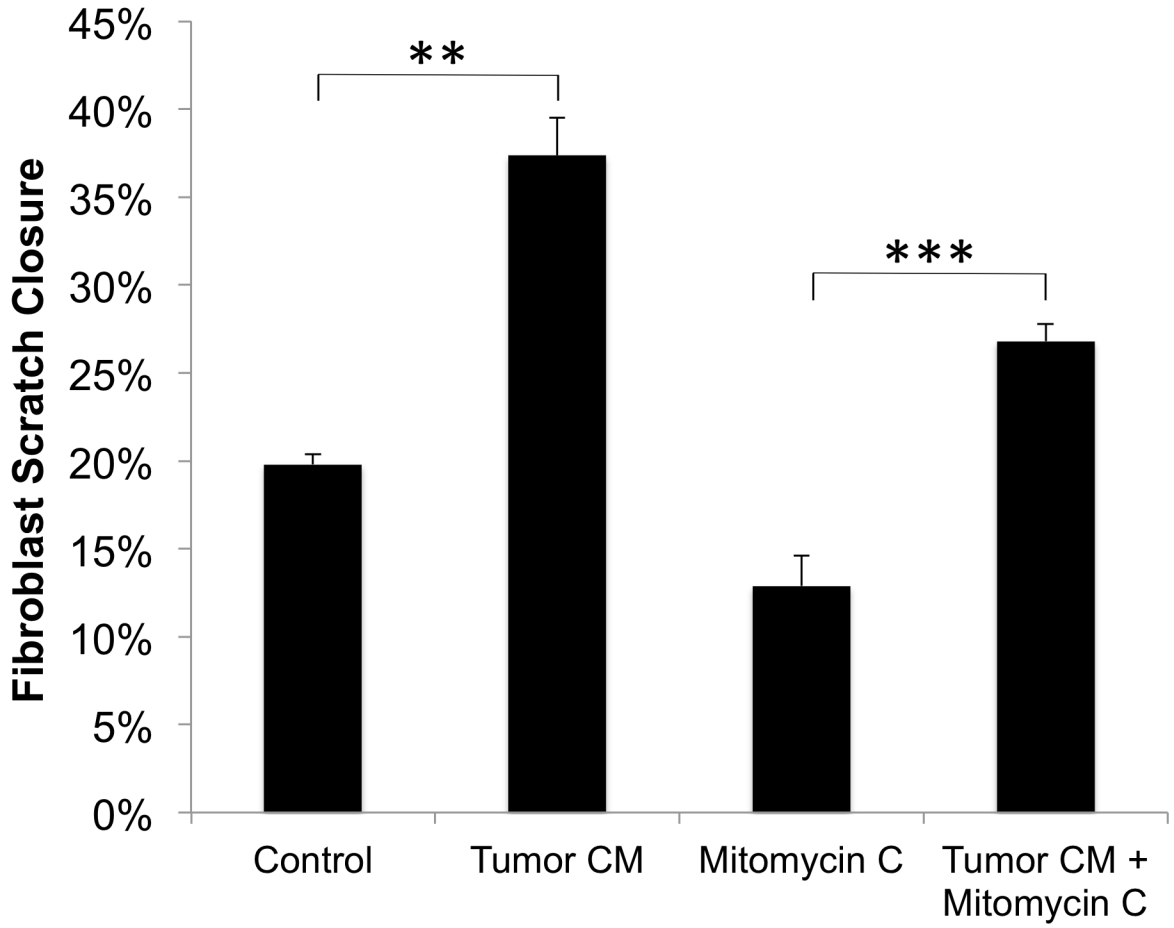

Figure 4.11. Tumor factors increase fibroblast migration even when proliferation is inhibited. Fibroblast monolayers were treated with serum free media or mitomycin C prior to performing scratch wound healing assays in serum free media or tumor conditioned media. ** = $p<0.01$, *** = $p<0.005$.

Because tumor conditioned media not only appears to enhance fibroblast migration, but to also enhance fibroblast proliferation, it is possible that the apparent increase in migration is just an artifact of more fibroblasts being present in the monolayer. If this is the case, then the increase in migration would no longer occur if proliferation were inhibited. On the contrary, fibroblast monolayers that were treated with mitomycin C before starting the scratch wound healing assay still exhibited increased migration in

tumor conditioned media (Fig. 4.11). Thus, tumor factors truly stimulate fibroblast migration and also fibroblast proliferation.

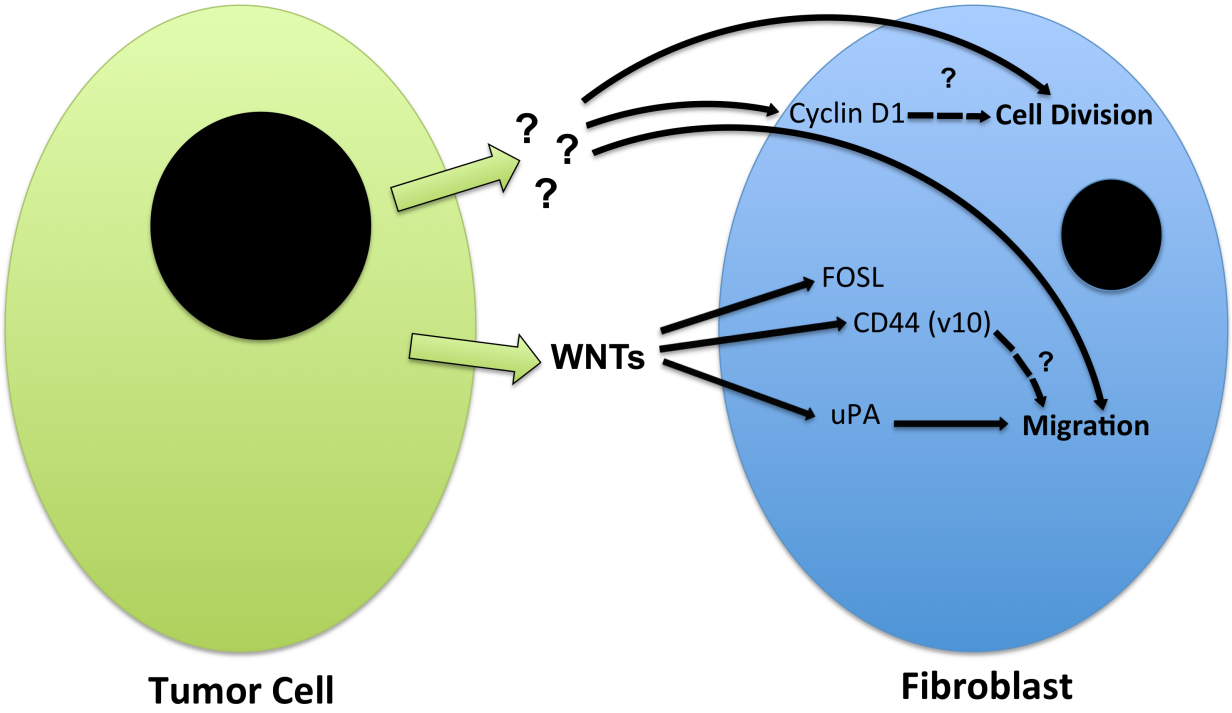

Figure 4.12. Schematic of tumor influence on fibroblast migration and proliferation. Tumor cells stimulate fibroblast migration and proliferation through WNT-dependent and WNT-independent mechanisms.

Together, the results of this study provide considerable insight into tumor-stromal fibroblast interactions. Tumor-derived WNT ligands, possibly WNT 10A or WNT11, activate canonical WNT signaling in fibroblasts, which upregulates uPA expression and uPA activity regulates migration (Fig. 4.12). This activation of WNT signaling in fibroblasts also upregulates FOSL and CD44 expression. Specifically, CD44 transcripts containing variant exon v10 are upregulated by tumor factors and could possibly contribute to enhancing migration in conjunction with uPA. Other tumor-derived factors are required and act in synergy with the WNT ligands to increase fibroblast migration. Also, non-WNT tumor factors increase cell division potentially by upregulating cyclin D1.

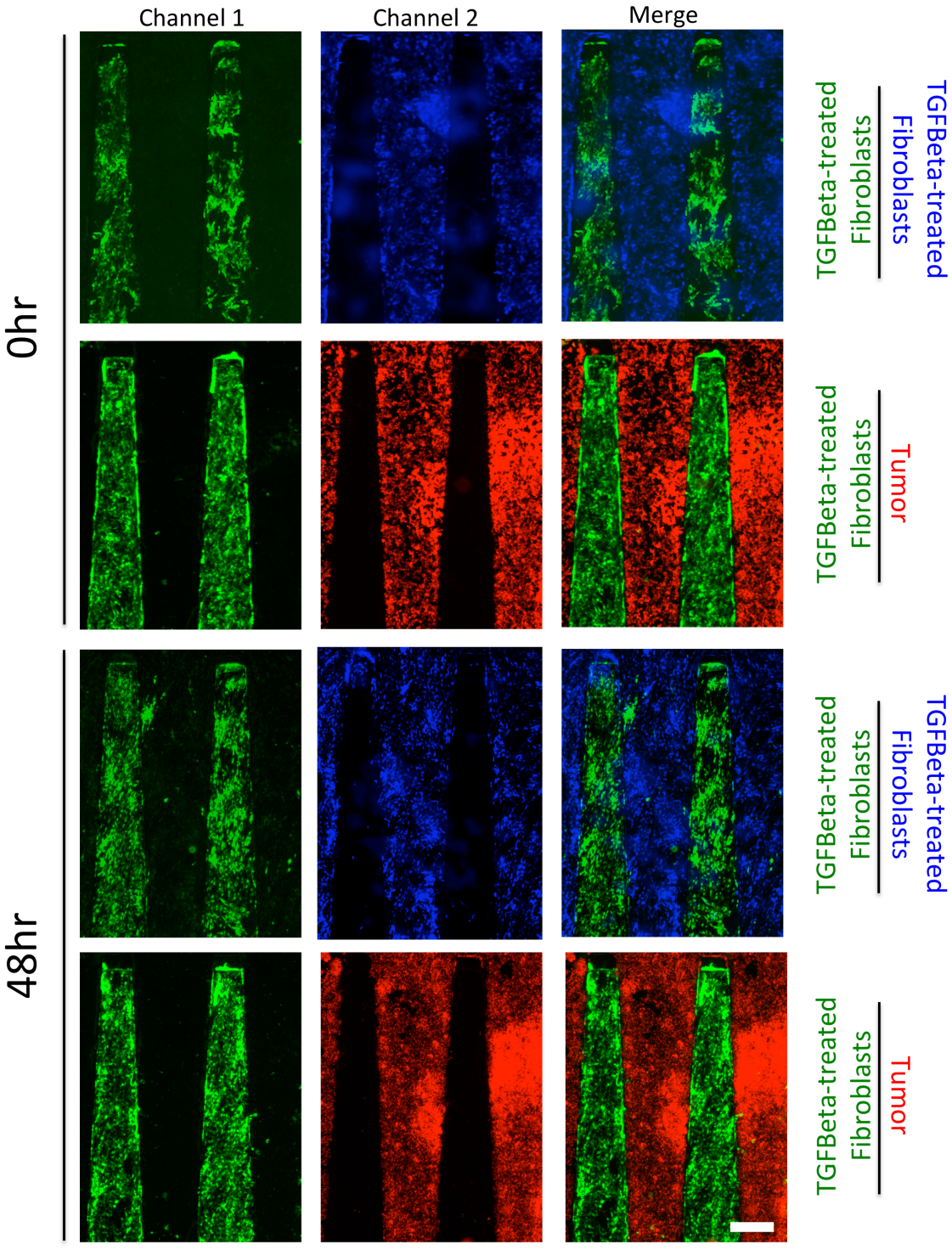

Figure 4.13. Fibroblasts invasion into tumor cells is greater than invasion into other fibroblasts. Fibroblasts (green) were co-cultured with other fibroblasts (blue) or with tumor cells (red) for 48hr on combs in the contact mode. More fibroblasts migrated onto the comb containing tumor cells as indicated by a higher number of green cells among red cells compared to green cells among blue cells.

In addition to studying the fibroblast response to tumor cell signals, we also began to investigate the effect of TGFβ treatment to activate fibroblasts. The colon fibroblasts that had been activated by TGFβ treatment prior to contact comb co-culture appeared to move less in general and did not invade the adjacent TGFβ-activated fibroblast comb or tumor cell comb much at all (Fig. 4.13). Likewise, compared to untreated fibroblasts, TGFβ-activated fibroblasts were less effective at closing the scratch in a scratch wound healing assay in both control media and tumor conditioned media (Fig. 4.14).

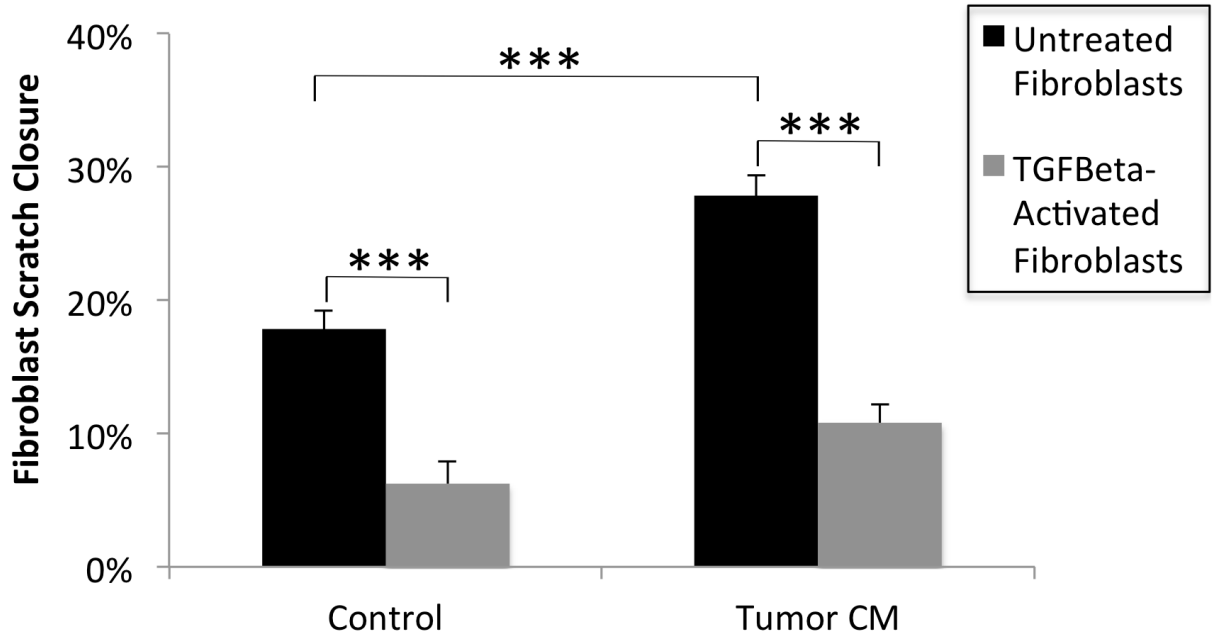

Figure 4.14. Untreated fibroblasts migrate more than TGFβ-treated fibroblasts. Untreated fibroblasts and TGFβ-treated fibroblasts were cultured in monolayers and subjected to scratch assays in the presence of serum-free media or tumor conditioned media (CM). *** = $p < 0.005$.

By identifying differences in gene expression between TGFβ-treated fibroblasts and untreated fibroblasts, GSEA analysis determined that TGFβ treatment appeared to affect the expression of WNT pathway components. WNT5a, Frizzled 8 (FZD8), and Cyclin D1, for example, were identified as being upregulated in TGFβ-activated fibroblasts, while WNT2B and uPA were identified as downregulated genes (data not shown). Further investigation is still needed, but it appears that TGFβ treatment may inhibit fibroblast migration by downregulating uPA expression, since uPA activity was shown to mediate fibroblast migration earlier in this chapter (Fig. 4.8) and in previous studies.[66] Similarly, since WNT5A and FZD8 are upregulated by TGFβ treatment, it is also possible that WNT5A-FZD8 autocrine signaling is involved in this effect because there is evidence that TGFβ induces WNT5a-FZD8 signaling in smooth muscle cells[76] and that WNT5a and FZD8 expression inhibits migration of breast cancer cells and convergent extension in Xenopus embryos.[77,78]

4.5 Discussion

A tremendous amount of focus has been placed on investigating tumor cell migration, invasion, and metastasis and identifying the role that stromal cells in the tumor microenvironment play in these events. By comparison, very little attention has been applied to determining how stromal cells, especially fibroblasts, appear there in the first place to make those interactions possible. Understanding the mechanisms behind this may be just as important, however, because it could provide additional and potentially effective therapeutic targets. Among the work that has been done in this area, one group used a live, *in vivo* imaging platform to watch as desmin-positive fibroblast-like cells infiltrated colon cancer liver metastases overtime as if they were being recruited by the tumor cells.[61] Additional studies have identified TGFβ, PDGF, other growth factors, and cytokines as the

chemotactic signals involved in tumor cell recruitment of fibroblasts.[59] Very recently, in a mouse mammary carcinoma model, tumor-derived WNT7A mediated the recruitment and activation of fibroblasts, but it did not operate through the canonical WNT pathway.[79] Rather, WNT7A appeared to indirectly exert its effect by promoting TGFβ receptor signaling.[79] Thus, until now, there has been no evidence showing that tumor cells induce fibroblast migration through canonical WNT signaling.

As mentioned previously, it is known that the WNT pathway can regulate cellular movement. There is also evidence that it can stimulate fibroblast migration in a number of contexts outside of cancer,[80-82] however, tumor-initiated canonical WNT-dependent fibroblast migration has never been reported. In cancer, canonical WNT pathway activity is most commonly associated with tumor cells and is known to be a potent regulator of tumor growth, survival, progression, and metastasis.[64] Here we showed that tumor cells trigger fibroblast migration using the canonical WNT pathway and that this interaction requires uPA activity. Interestingly, uPA is a marker of breast cancer stromal cells and its expression correlates with tumor progression,[83] so our results provide a possible explanation for this *in vivo* data. Specifically, upregulation of uPA expression may lead to higher fibroblast migration into the tumor microenvironment, where they then communicate with tumor and other stromal cells to encourage tumor progression. Tumor factors also significantly increased fibroblast proliferation, through WNT-independent mechanisms, which correlates with findings that fibroblasts at the edge of colorectal tumors are more proliferative than in normal tissue[84] and supports the theory that the tumor not only recruits fibroblasts to the microenvironment, but also increases fibroblast abundance there by stimulating them to proliferate.[84] Likewise, we found that uPA

expression was downregulated in colon fibroblasts activated with TGFβ to mimic myofibroblasts, which matches the results of a study with corneal and breast fibroblasts.[85,86] Loss of uPA expression could be the cause of reduced migration in TGFβ-activated fibroblasts. Another live, in vivo imaging system enabled Egeblad et al. (2008) to observe fibroblasts migrating into the tumor microenvironment and to discover that they are more mobile in the periphery of the tumor and less migratory in the tumor mass. Based on this and other evidence, the idea that tumors communicate with fibroblasts to first attract them and then make them stay nearby so that they can contribute to tumor survival and mestastasis[88] is starting to gain supporters. Our data suggests that this is possible and that cancer cells use canonical WNT signaling to attract fibroblasts and then activate them through TGFβ signaling to become less-migratory myofibroblasts that can promote cancer progression.

In summary, our study provides the first evidence of canonical WNT-dependent tumor-induced fibroblast migration and begins to elucidate the mechanism through which it occurs. Recruitment of fibroblasts into the tumor microenvironment was previously understudied compared to stromal-mediated tumor progression, but this early event in tumor development could yield successful drug targets if we better understand the interactions that it involves.

4.6 Supplementary Information

Gene	Forward 5' to 3'	Reverse 5' to 3'
HPRT	GACCAGTCAACAGGGGACA	GTGTCAATTATATCTTCCACAA
uPA	TCGCTCAAGGCTTAACTCCAACAC	CCCAGCTCACAATTCCAGTCAAAG
FOSL	ATCAGCCCGGAGGAAGAGGAG	CAGGCTGGGGGTGAAAGGAGT
CD44	GACACCATGGACAAGTTTTGG	GAGATGCTGTAGCGACCATT
CD44v4	ACCACACCACGGGCTTTTGACC	GGGTTCCACTGGGTCCAGTCCT
CD44v6	AGGAACAGTGGTTTGGCAAC	CGAATGGGAGTCTTCTCTGG
CD44v8	TCAGCCTACTGCAAATCCAA	GAGGTCCTGTCCTGTCCAAA
CD44v10	GGAATGATGTCACAGGTGGA	AGGTCACTGGGATGAAGGTC
Cyclin D1	GTGTCCTACTTCAAATGTGTGC	AGCGGTCCAGGTAGTTCA

Table S4.1. Primer sequences employed for qRT-PCR. These were employed for the validation experiments and may be different from the primers in the qRT-PCR arrays.

4.7 Acknowledgements

This work was supported by the Chao Family Comprehensive Cancer Center through NCI Center Grant (P30A062203) and the American Cancer Society (ACS/IRG 98-279-07). K.H.S was supported by fellowships from the NSF (GRFP) and the NIH (T32-HD060555).

CONCLUSION

Development, tissue homeostasis, and disease are all orchestrated through complex communication among spatially organized cell populations. The key to understanding these processes and knowing how to effectively manipulate them for therapeutic or scientific purposes lies in thoroughly studying the cell-cell interactions involved. Simple in-vitro cell cultures can provide great insight into these mechanisms. However, some methods may not be sensitive to short-range communication and, at the same time, allow one to easily study the dynamic responses of each population of cells to co-culture. In contrast, the comb platform does possess this sensitivity and has significantly expanded our understanding of the communication required hepatocyte function, myoblast differentiation, and adipose stem cell differentiation.

In this work, we have also shown that the comb platform can be adapted to provide an experimental model of morphogen-dependent border formation in development, a new method of maintaining stem cells that enables easy purification of mES from culture with feeder cells, and a screening system to detect and identify short-range paracrine interactions. We demonstrate that BMP causes cortical precursor cells to differentiate toward a neuronal cell fate and to migrate. In addition, we show that maintenance of pluripotency markers in feeder-dependent mouse embryonic stem cells may not need direct contact with feeders, as previously thought, but instead only require close-range paracrine communication with them. Finally, we provide the first evidence that tumor cells stimulate fibroblast migration through a mechanism that involves canonical WNT signaling. An even deeper understanding of the cell-cell interactions involved in these biological systems can be acquired through continued use of the comb co-culture. More importantly,

however, the unique features and versatility of the comb platform make it a valuable tool for studying communication in other cellular contexts could significantly impact multiple areas of biology.

References

1. Fortini, M. E. (2009). Notch signaling: the core pathway and its posttranslational regulation. *Developmental Cell*, *16*(5), 633–47.
2. Halbleib, J. M., & Nelson, W. J. (2006). Cadherins in development: cell adhesion, sorting, and tissue morphogenesis. *Genes & Development*, *20*(23), 3199–214.
3. Williams, E. J., Furness, J., Walsh, F. S., & Doherty, P. (1994). Activation of the FGF receptor underlies neurite outgrowth stimulated by L1, N-CAM, and N-cadherin. *Neuron*, *13*(3), 583–594.
4. Goodenough, D. A., & Paul, D. L. (2009). Gap junctions. *Cold Spring Harbor Perspectives in Biology*, *1*(1), a002576.
5. Wei, C.-J., Xu, X., & Lo, C. W. (2004). Connexins and cell signaling in development and disease. *Annual Review of Cell and Developmental Biology*, *20*, 811–38.
6. Naus, C. C., & Laird, D. W. (2010). Implications and challenges of connexin connections to cancer. *Nature Reviews. Cancer*, *10*(6), 435–41.
7. Harburger, D. S., & Calderwood, D. A. (2009). Integrin signalling at a glance. *Journal of Cell Science*, *122*(Pt 2), 159–63.
8. Freinbichler, W., Colivicchi, M. A., Stefanini, C., Bianchi, L., Ballini, C., Misini, B., … Della Corte, L. (2011). Highly reactive oxygen species: detection, formation, and possible functions. *Cellular and Molecular Life Sciences : CMLS*, *68*(12), 2067–79.
9. Fuerer, C., Nostro, M. C., & Constam, D. B. (2014). Nodal·Gdf1 heterodimers with bound prodomains enable serum-independent nodal signaling and endoderm differentiation. *The Journal of Biological Chemistry*, *289*(25), 17854–71.
10. Powers, C. J., McLeskey, S. W., & Wellstein, A. (2000). Fibroblast growth factors, their receptors and signaling. *Endocrine-Related Cancer*, *7*(3), 165–97.
11. Port, F., & Basler, K. (2010). Wnt trafficking: new insights into Wnt maturation, secretion and spreading. *Traffic (Copenhagen, Denmark)*, *11*(10), 1265–71.
12. Bhatia, S. N., Balis, U. J., Yarmush, M. L., & Toner, M. (1999). Effect of cell-cell interactions in preservation of cellular phenotype: cocultivation of hepatocytes and nonparenchymal cells. *FASEB J*, *13*(14), 1883–1900.
13. Hui, E. E., & Bhatia, S. N. (2007). Micromechanical control of cell-cell interactions. *Proceedings of the National Academy of Sciences of the United States of America*, *104*(14), 5722–6.
14. Rao, N., Evans, S., Stewart, D., Spencer, K. H., Sheikh, F., Hui, E. E., & Christman, K. L. (2012). Fibroblasts influence muscle progenitor differentiation and alignment in contact independent and dependent manners in organized co-culture devices. *Biomedical Microdevices*. doi:10.1007/s10544-012-9709-9
15. Rao, N., Grover, G., Vincent, L. G., Evans, S. C., Choi, Y. S., Spencer, K., … Christman, K. (2013). A co-culture device with a tunable stiffness to understand combinatorial cell-cell and cell-matrix interactions. *Integrative Biology*. doi:10.1039/c3ib40078f
16. Spencer, K. H., Kim, M. Y., Hughes, C. C. W., & Hui, E. E. (2014). A screen for short-range paracrine interactions. *Integrative Biology : Quantitative Biosciences from Nano to Macro*, *6*(4), 382–7.

17. Tan, J. L., Liu, W., Nelson, C. M., Raghavan, S., & Chen, C. S. (2004). Simple approach to micropattern cells on common culture substrates by tuning substrate wettability. *Tissue Engineering*, *10*(5-6), 865–72.
18. Tien, J., Nelson, C. M., & Chen, C. S. (2002). Fabrication of aligned microstructures with a single elastomeric stamp. *Proceedings of the National Academy of Sciences of the United States of America*, *99*(4), 1758–62.
19. Kaji, H., Camci-Unal, G., Langer, R., & Khademhosseini, A. (2011). Engineering systems for the generation of patterned co-cultures for controlling cell-cell interactions. *Biochimica et Biophysica Acta*, *1810*(3), 239–50.
20. Folch, A., Jo, B. H., Hurtado, O., Beebe, D. J., & Toner, M. (2000). Microfabricated elastomeric stencils for micropatterning cell cultures. *Journal of Biomedical Materials Research*, *52*(2), 346–53.
21. Ostuni, E., Kane, R., Chen, C. S., Ingber, D. E., & Whitesides, G. M. (2000). Patterning Mammalian Cells Using Elastomeric Membranes. *Langmuir*, *16*(20), 7811–7819.
22. Wright, D., Rajalingam, B., Karp, J. M., Selvarasah, S., Ling, Y., Yeh, J., … Khademhosseini, A. (2008). Reusable, reversibly sealable parylene membranes for cell and protein patterning. *Journal of Biomedical Materials Research. Part A*, *85*(2), 530–8.
23. Wright, D., Rajalingam, B., Selvarasah, S., Dokmeci, M. R., & Khademhosseini, A. (2007). Generation of static and dynamic patterned co-cultures using microfabricated parylene-C stencils. *Lab on a Chip*, *7*(10), 1272–9.
24. Chen, Q., Wu, J., Zhuang, Q., Lin, X., Zhang, J., & Lin, J.-M. (2013). Microfluidic isolation of highly pure embryonic stem cells using feeder-separated co-culture system. *Scientific Reports*, *3*, 2433.
25. Domenech, M., Bjerregaard, R., Bushman, W., & Beebe, D. J. (2012). Hedgehog signaling in myofibroblasts directly promotes prostate tumor cell growth. *Integrative Biology : Quantitative Biosciences from Nano to Macro*, *4*(2), 142–52.
26. Torisawa, Y., Mosadegh, B., Luker, G. D., Morell, M., O'Shea, K. S., & Takayama, S. (2009). Microfluidic hydrodynamic cellular patterning for systematic formation of co-culture spheroids. *Integrative Biology : Quantitative Biosciences from Nano to Macro*, *1*(11-12), 649–54.
27. Stevens, K. R., Ungrin, M. D., Schwartz, R. E., Ng, S., Carvalho, B., Christine, K. S., … Bhatia, S. N. (2013). InVERT molding for scalable control of tissue microarchitecture. *Nature Communications*, *4*, 1847.
28. Gartner, Z. J., & Bertozzi, C. R. (2009). Programmed assembly of 3-dimensional microtissues with defined cellular connectivity. *Proceedings of the National Academy of Sciences of the United States of America*, *106*(12), 4606–10.
29. Srinivasan, S., Hu, J. S., Currle, D. S., Fung, E. S., Hayes, W. B., Lander, A. D., & Monuki, E. S. (2014). A BMP-FGF Morphogen Toggle Switch Drives the Ultrasensitive Expression of Multiple Genes in the Developing Forebrain. PLoS Computational Biology, 10(2), e1003463.
30. Hui, E. E., Li, C., Agrawal, A., & Bhatia, S. N. (2014). Macro-to-Micro Interface for the Control of Cellular Organization. *Journal of Microelectromechanical Systems*, *23*(2), 391–397.

31. March, S., Hui, E. E., Underhill, G. H., Khetani, S., & Bhatia, S. N. (2009). Microenvironmental regulation of the sinusoidal endothelial cell phenotype *in vitro*. *Hepatology (Baltimore, Md.)*, *50*(3), 920–8.
32. Hu, J. S., Doan, L. T., Currle, D. S., Paff, M., Rheem, J. Y., Schreyer, R., … Monuki, E. S. (2008). Border formation in a Bmp gradient reduced to single dissociated cells. *Proceedings of the National Academy of Sciences of the United States of America*, *105*(9), 3398–403.
33. Doan, L. T., Javier, A. L., Furr, N. M., Nguyen, K. L., Cho, K. W., & Monuki, E. S. (2012). A Bmp reporter with ultrasensitive characteristics reveals that high Bmp signaling is not required for cortical hem fate. *PloS One*, *7*(9), e44009.
34. Currle, D. S., Cheng, X., Hsu, C.-M., & Monuki, E. S. (2005). Direct and indirect roles of CNS dorsal midline cells in choroid plexus epithelia formation. *Development (Cambridge, England)*, *132*(15), 3549–59.
35. De Chaumont, F., Dallongeville, S., Chenouard, N., Hervé, N., Pop, S., Provoost, T., … Olivo-Marin, J.-C. (2012). Icy: an open bioimage informatics platform for extended reproducible research. *Nature Methods*, *9*(7), 690–6.
36. Segklia, A., Seuntjens, E., Elkouris, M., Tsalavos, S., Stappers, E., Mitsiadis, T. A., … Graf, D. (2012). Bmp7 regulates the survival, proliferation, and neurogenic properties of neural progenitor cells during corticogenesis in the mouse. *PloS One*, *7*(3), e34088.
37. Martin, G. R. (1981). Isolation of a pluripotent cell line from early mouse embryos cultured in medium conditioned by teratocarcinoma stem cells. *Proceedings of the National Academy of Sciences of the United States of America*, *78*(12), 7634–8.
38. Evans, M. J., & Kaufman, M. H. (1981). Establishment in culture of pluripotential cells from mouse embryos. *Nature*, *292*(5819), 154–156.
39. Silva, J., & Smith, A. (2008). Capturing pluripotency. *Cell*, *132*(4), 532–6.
40. Pera, M. F., & Tam, P. P. L. (2010). Extrinsic regulation of pluripotent stem cells. *Nature*, *465*(7299), 713–20.
41. Li, Z., Barron, M. R., Lough, J., & Zhao, M. (2008). Rapid single-step separation of pluripotent mouse embryonic stem cells from mouse feeder fibroblasts. *Stem Cells and Development*, *17*(2), 383–7.
42. Hwang, S.-T., Kang, S.-W., Lee, S.-J., Lee, T.-H., Suh, W., Shim, S. H., … Lee, S.-H. (2010). The expansion of human ES and iPS cells on porous membranes and proliferating human adipose-derived feeder cells. *Biomaterials*, *31*(31), 8012–21..031
43. Kim, S., Ahn, S. E., Lee, J. H., Lim, D.-S., Kim, K.-S., Chung, H.-M., & Lee, S.-H. (2007). A novel culture technique for human embryonic stem cells using porous membranes. *Stem Cells (Dayton, Ohio)*, *25*(10), 2601–9.
44. Dong, F. L., Kaleri, H. A., Lu, Y. D., Song, C. L., Jiang, B. C., Zhang, B. L., … Liu, H. L. (2012). Generation of induced pluripotent mouse stem cells in an indirect co-culture system. *Genetics and Molecular Research : GMR*, *11*(4), 4179–86..6.1
45. Qi, X., Li, T.-G., Hao, J., Hu, J., Wang, J., Simmons, H., … Zhao, G.-Q. (2004). BMP4 supports self-renewal of embryonic stem cells by inhibiting mitogen-activated protein kinase pathways. *Proceedings of the National Academy of Sciences of the United States of America*, *101*(16), 6027–32.
46. Ohkawara, B., Iemura, S., ten Dijke, P., & Ueno, N. (2002). Action range of BMP is defined by its N-terminal basic amino acid core. *Current Biology : CB*, *12*(3), 205–9.

47. Hao, J., Li, T.-G., Qi, X., Zhao, D.-F., & Zhao, G.-Q. (2006). WNT/beta-catenin pathway up-regulates Stat3 and converges on LIF to prevent differentiation of mouse embryonic stem cells. *Developmental Biology*, *290*(1), 81–91.
48. Melen, G. J., Levy, S., Barkai, N., & Shilo, B.-Z. (2005). Threshold responses to morphogen gradients by zero-order ultrasensitivity. *Molecular Systems Biology*, *1*, 2005.0028.
49. Winterbourn, C. C. (2008). Reconciling the chemistry and biology of reactive oxygen species. *Nature Chemical Biology*, *4*(5), 278–86.
50. Domenech, M., Bjerregaard, R., Bushman, W., & Beebe, D. J. (2012). Hedgehog signaling in myofibroblasts directly promotes prostate tumor cell growth. *Integrative Biology : Quantitative Biosciences from Nano to Macro*, *4*(2), 142–52.
51. Yamamoto, N., Yang, M., Jiang, P., Xu, M., Tsuchiya, H., Tomita, K., … Hoffman, R. M. (2003). Determination of Clonality of Metastasis by Cell-Specific Color-Coded Fluorescent-Protein Imaging. *Cancer Res.*, *63*(22), 7785–7790.
52. Engl, T., Relja, B., Blumenberg, C., Müller, I., Ringel, E. M., Beecken, W.-D., … Blaheta, R. A. (2006). Prostate tumor CXC-chemokine profile correlates with cell adhesion to endothelium and extracellular matrix. *Life Sciences*, *78*(16), 1784–93.
53. Bièche, I., Chavey, C., Andrieu, C., Busson, M., Vacher, S., Le Corre, L., … Lazennec, G. (2007). CXC chemokines located in the 4q21 region are up-regulated in breast cancer. *Endocrine-Related Cancer*, *14*(4), 1039–52.
54. Owen, J. D., Strieter, R., Burdick, M., Haghnegahdar, H., Nanney, L., Shattuck-Brandt, R., & Richmond, A. (1997). Enhanced tumor-forming capacity for immortalized melanocytes expressing melanoma growth stimulatory activity/growth-regulated cytokine beta and gamma proteins. *International Journal of Cancer. Journal International Du Cancer*, *73*(1), 94–103.
55. Stratman, A. N., Malotte, K. M., Mahan, R. D., Davis, M. J., & Davis, G. E. (2009). Pericyte recruitment during vasculogenic tube assembly stimulates endothelial basement membrane matrix formation. *Blood*, *114*(24), 5091–101.
56. Jørgensen, C., Sherman, A., Chen, G. I., Pasculescu, A., Poliakov, A., Hsiung, M., … Pawson, T. (2009). Cell-specific information processing in segregating populations of Eph receptor ephrin-expressing cells. *Science (New York, N.Y.)*, *326*(5959), 1502–9.
57. Gauthier, N. P., Soufi, B., Walkowicz, W. E., Pedicord, V. A., Mavrakis, K. J., Macek, B., … Miller, M. L. (2013). Cell-selective labeling using amino acid precursors for proteomic studies of multicellular environments. *Nature Methods*, *10*(8), 768–73.
58. Miller, M. R., Robinson, K. J., Cleary, M. D., & Doe, C. Q. (2009). TU-tagging: cell type-specific RNA isolation from intact complex tissues. *Nature Methods*, *6*(6), 439–41.
59. Kalluri, R., & Zeisberg, M. (2006). Fibroblasts in cancer. *Nature Reviews. Cancer*, *6*(5), 392–401.
60. Bhowmick, N. A., Neilson, E. G., & Moses, H. L. (2004). Stromal fibroblasts in cancer initiation and progression. *Nature*, *432*(7015), 332–7.
61. Suetsugu, A., Osawa, Y., Nagaki, M., Saji, S., Moriwaki, H., Bouvet, M., & Hoffman, R. M. (2011). Imaging the recruitment of cancer-associated fibroblasts by liver-metastatic colon cancer. *Journal of Cellular Biochemistry*, *112*(3), 949–53.

62. Ishii, G., Sangai, T., Oda, T., Aoyagi, Y., Hasebe, T., Kanomata, N., … Ochiai, A. (2003). Bone-marrow-derived myofibroblasts contribute to the cancer-induced stromal reaction. *Biochemical and Biophysical Research Communications*, *309*(1), 232–40.
63. Subramanian, A., Tamayo, P., Mootha, V. K., Mukherjee, S., Ebert, B. L., Gillette, M. A., … Mesirov, J. P. (2005). Gene set enrichment analysis: a knowledge-based approach for interpreting genome-wide expression profiles. *Proceedings of the National Academy of Sciences of the United States of America*, *102*(43), 15545–50.
64. Anastas, J. N., & Moon, R. T. (2013). WNT signalling pathways as therapeutic targets in cancer. *Nature Reviews. Cancer*, *13*(1), 11–26.
65. Bekes, E. M., Deryugina, E. I., Kupriyanova, T. A., Zajac, E., Botkjaer, K. A., Andreasen, P. A., & Quigley, J. P. (2011). Activation of pro-uPA is critical for initial escape from the primary tumor and hematogenous dissemination of human carcinoma cells. *Neoplasia (New York, N.Y.)*, *13*(9), 806–21.
66. Weaver, A. M., Hussaini, I. M., Mazar, A., Henkin, J., & Gonias, S. L. (1997). Embryonic fibroblasts that are genetically deficient in low density lipoprotein receptor-related protein demonstrate increased activity of the urokinase receptor system and accelerated migration on vitronectin. *The Journal of Biological Chemistry*, *272*(22), 14372–9.
67. Carlin, S. M., Resink, T. J., Tamm, M., & Roth, M. (2005). Urokinase signal transduction and its role in cell migration. *FASEB Journal : Official Publication of the Federation of American Societies for Experimental Biology*, *19*(2), 195–202.
68. Rao, J. S., Gujrati, M., & Chetty, C. (2013). Tumor-associated soluble uPAR-directed endothelial cell motility and tumor angiogenesis. *Oncogenesis*, *2*, e53.
69. Galindo, C. L., Fadl, A. A., Sha, J., Pillai, L., Gutierrez, C., & Chopra, A. K. (2005). Microarray and proteomics analyses of human intestinal epithelial cells treated with the Aeromonas hydrophila cytotoxic enterotoxin. *Infection and Immunity*, *73*(5), 2628–43.
70. Rumantir, R. A. (2013). The Requirement for Oxygen in the Maturation and Secretion of Soluble urokinase Plasminogen Activator Receptor (uPAR). University of Toronto. Retrieved from http://oatd.org/oatd/record?record=handle%5C:1807%5C%2F43321
71. Takeuchi, K., Yamaguchi, A., Urano, T., Goi, T., Nakagawara, G., & Shiku, H. (1995). Expression of CD44 Variant Exons 8-10 in Colorectal Cancer and Its Relationship to Metastasis. *Cancer Science*, *86*(3), 292–297.
72. Iida, J., Clancy, R., Dorchak, J., Somiari, R. I., Somiari, S., Cutler, M. Lou, … Shriver, C. D. (2014). DNA aptamers against exon v10 of CD44 inhibit breast cancer cell migration. *PloS One*, *9*(2), e88712.
73. Wang, S. J., Wong, G., de Heer, A.-M., Xia, W., & Bourguignon, L. Y. W. (2009). CD44 variant isoforms in head and neck squamous cell carcinoma progression. *The Laryngoscope*, *119*(8), 1518–30.
74. Yoshinari, C., Mizusawa, N., Byers, H. R., & Akasaka, T. (1999). CD44 variant isoform CD44v10 expression of human melanoma cell lines is upregulated by hyaluronate and correlates with migration. *Melanoma Research*, *9*(3), 223–31.
75. Katagiri, Y. U., Sleeman, J., Fujii, H., Herrlich, P., Hotta, H., Tanaka, K., … Uede, T. (1999). CD44 variants but not CD44s cooperate with beta1-containing integrins to

permit cells to bind to osteopontin independently of arginine-glycine-aspartic acid, thereby stimulating cell motility and chemotaxis. *Cancer Research*, *59*(1), 219–26.
76. Kumawat, K., Menzen, M. H., Bos, I. S. T., Baarsma, H. A., Borger, P., Roth, M., … Gosens, R. (2013). Noncanonical WNT-5A signaling regulates TGF-β-induced extracellular matrix production by airway smooth muscle cells. *FASEB Journal : Official Publication of the Federation of American Societies for Experimental Biology*, *27*(4), 1631–43.
77. Jiang, W., Crossman, D. K., Mitchell, E. H., Sohn, P., Crowley, M. R., & Serra, R. (2013). WNT5A inhibits metastasis and alters splicing of Cd44 in breast cancer cells. *PloS One*, *8*(3), e58329.
78. Wallingford, J. B., Vogeli, K. M., & Harland, R. M. (2001). Regulation of convergent extension in Xenopus by Wnt5a and Frizzled-8 is independent of the canonical Wnt pathway. *The International Journal of Developmental Biology*, *45*(1), 225–7.
79. Avgustinova, A., Iravani, M., Calvo, F., Sahai, E., Klingbeil, P., & Isacke, C. (2014). Abstract SY21-03: Fibroblast recruitment and activation in breast cancer progression. *Cancer Res.*, *74*(19_Supplement), SY21–03–. doi:10.1158/1538-7445.AM2014-SY21-03
80. Laeremans, H., Rensen, S. S., Ottenheijm, H. C. J., Smits, J. F. M., & Blankesteijn, W. M. (2010). Wnt/frizzled signalling modulates the migration and differentiation of immortalized cardiac fibroblasts. *Cardiovascular Research*, *87*(3), 514–23.
81. Wei, J., Fang, F., Lam, A. P., Sargent, J. L., Hamburg, E., Hinchcliff, M. E., … Varga, J. (2012). Wnt/β-catenin signaling is hyperactivated in systemic sclerosis and induces Smad-dependent fibrotic responses in mesenchymal cells. *Arthritis and Rheumatism*, *64*(8), 2734–45.
82. Poon, R., Nik, S. A., Ahn, J., Slade, L., & Alman, B. A. (2009). Beta-catenin and transforming growth factor beta have distinct roles regulating fibroblast cell motility and the induction of collagen lattice contraction. *BMC Cell Biology*, *10*(1), 38.
83. Dublin, E., Hanby, A., Patel, N. K., Liebman, R., & Barnes, D. (2000). Immunohistochemical expression of uPA, uPAR, and PAI-1 in breast carcinoma. Fibroblastic expression has strong associations with tumor pathology. *The American Journal of Pathology*, *157*(4), 1219–27.
84. Sivridis, E., Giatromanolaki, A., & Koukourakis, M. I. (2005). Proliferating fibroblasts at the invading tumour edge of colorectal adenocarcinomas are associated with endogenous markers of hypoxia, acidity, and oxidative stress. *Journal of Clinical Pathology*, *58*(10), 1033–8.
85. Bernstein, A. M., Twining, S. S., Warejcka, D. J., Tall, E., & Masur, S. K. (2007). Urokinase receptor cleavage: a crucial step in fibroblast-to-myofibroblast differentiation. *Molecular Biology of the Cell*, *18*(7), 2716–27.
86. Sieuwerts, A. M., Klijn, J. G., Henzen-Logmand, S. C., Bouwman, I., Van Roozendaal, K. E., Peters, H. A., … Foekens, J. A. (1998). Urokinase-type-plasminogen-activator (uPA) production by human breast (myo) fibroblasts *in vitro*: influence of transforming growth factor-beta(1) (TGF beta(1)) compared with factor(s) released by human epithelial-carcinoma cells. *International Journal of Cancer. Journal International Du Cancer*, *76*(6), 829–35.
87. Egeblad, M., Ewald, A. J., Askautrud, H. A., Truitt, M. L., Welm, B. E., Bainbridge, E., … Werb, Z. (n.d.). Visualizing stromal cell dynamics in different tumor

microenvironments by spinning disk confocal microscopy. *Disease Models & Mechanisms*, *1*(2-3), 155–67; discussion 165.

88. Rønnov-Jessen, L., & Petersen, O. W. (1993). Induction of alpha-smooth muscle actin by transforming growth factor-beta 1 in quiescent human breast gland fibroblasts. Implications for myofibroblast generation in breast neoplasia. *Laboratory Investigation; a Journal of Technical Methods and Pathology*, *68*(6), 696–707.